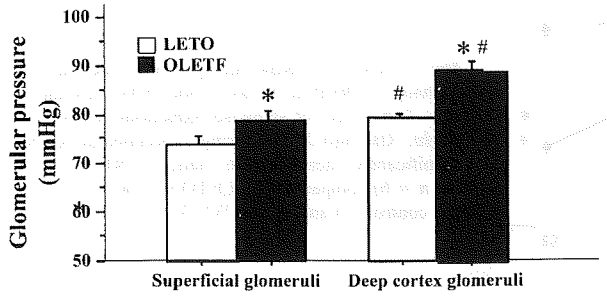

Fig. 6. Glomerular capillary pressure in superficial and juxtamedullary glomeruli in 30-wk LETO rats (n = 4) and OLETF rats (n = 4). $P < 0.05$ vs. LETO (*) and vs. superficial (#).

rats at 30–40 wk of age (Fig. 8). Although mean arterial pressure did not significantly change in the older rats, P_{sf} of OLETF rats (42.0 ± 2.0 mmHg) was significantly higher than that of LETO rats (36.0 ± 1.7 mmHg). Maximum activation of TGF caused P_{sf} at 40 nl/min in OLETF and LETO rats to fall to 39.4 ± 2.5 and to 29.0 ± 1.5 mmHg, respectively. Percent changes of zero perfusion values averaged −6.7 ± 3.1% in OLETF rats and −19.7 ± 1.5% in LETO rats ($P < 0.05$).

Renal pathology. Measurements of glomerular volume and sclerosis index for both strains of rats at 30–40 wk of age are summarized in Fig. 9. Although the tendency of a larger glomerular volume in the superficial cortex of OLETF rats did not reach significance, glomerular volume of juxtamedullary glomeruli was significantly greater in OLETF (2.17 ± 0.36 × 10^6 μm^3) than LETO (1.27 ± 0.06 × 10^6 μm^3) rats. Sclerosis index was significantly greater in OLETF than LETO rats in both surface (1.31 ± 0.12 vs. 0.68 ± 0.92) and deep cortical glomeruli (1.84 ± 0.12 vs. 0.99 ± 0.09). Moreover, regional comparisons showed significantly higher sclerosis index in deep cortical than in surface glomeruli in both strains of rats.

DISCUSSION

The present study was performed to assess autoregulatory and TGF responses of superficial and deep nephrons in type 2 diabetic OLETF rats. One of the important observations in the present study is that the ability of RBF autoregulation appears to be markedly reduced in the diabetic OLETF rats. RBF of OLETF rats fell almost linearly with a reduction of RPP, whereas an identical decrease of RPP had little effect on RBF in control LETO animals. The hemodynamic dysregulation of OLETF rats was more pronounced in the deep region of the renal cortex. Furthermore, impairment of autoregulation in OLETF rats was observed before the development of overt hyperglycemia, consistent with the notion that it may be a causal factor in diabetic nephropathy.

Autoregulation of RBF and glomerular filtration rate is thought to be mediated by at least two distinct mechanisms. One is a myogenic reaction that is intrinsic to all resistance vessels, whereas the second is a kidney-specific mechanism called TGF. Our present observations show that TGF abnormalities exist in OLETF rats and that they precede the rise of blood sugar and the development of diabetes. This raises the possibility that an abnormal TGF may be causally connected with the development of the hemodynamic abnormalities in the diabetes state. Abnormal TGF responsiveness has been reported previously in diabetes, especially in insulin-deficient states (8, 27). In addition, a dysfunction of voltage-dependent Ca^{2+} channels in vascular smooth muscle cells or an increased activation of ATP-dependent K^+ channels has been reported, suggesting that myogenic reactivity may be abnormal in diabetes as well (3). The diminished stability of RBF in the face of changes of RPP in STZ-induced diabetes in rats has been found to be improved by treatment with insulin (2, 5). Therefore, it is thought that not only insulin resistance but also hyperglycemia per se may affect autoregulation.

Glomeruli located close to the kidney surface differ in structure and function from those in the juxtamedullary region (8). Studies of regional hemodynamics have frequently used the Laser Doppler technology, although this approach only permits measurements of relative blood flow changes. Nevertheless, the Laser Doppler approach yields a continuous recording of blood flow velocity and is associated with comparatively minor disturbance of function. In the present study, we used this technique to evaluate autoregulation in the superficial and juxtamedullary regions of the kidney. In LETO rats, both surface and deep cortical blood flow was well regulated during an ~20 mmHg arterial pressure change, confirming previous reports using the same method (14–16). Whereas superficial cortical blood flow of OLETF rats was also well regulated, our data show for the first time that there is an autoregulation defect in the deep cortex in this type 2 diabetes model. The causes for the regional differences in autoregulatory abnormalities are unclear but could be related to changes of extracellular fluid volume and the renin-angiotensin system (16). It is also possible that distension of renal vessels resulting from the diabetic state may cause the autoregulation disability in the deep cortex.

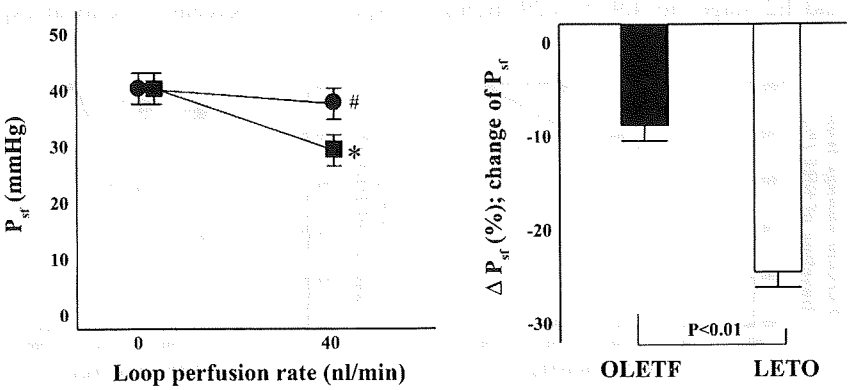

Fig. 7. Stop flow pressure (P_{sf}) and change in P_{sf} (ΔP_{sf}) in OLETF and LETO rats at 10–12 wk. *Left*: relationship between P_{sf} and rate of loop perfusion rate (0, 40 nl/min) with ATF in OLETF rats (●: n = 13) compared with those in LETO rats (■: n = 13). *Right*: %change of P_{sf} in OLETF rats (■: n = 13) compared with those in LETO rats (□: n = 13). $P < 0.05$ vs. P_{sf} at 0 nl/min (*) and vs. LETO (#).

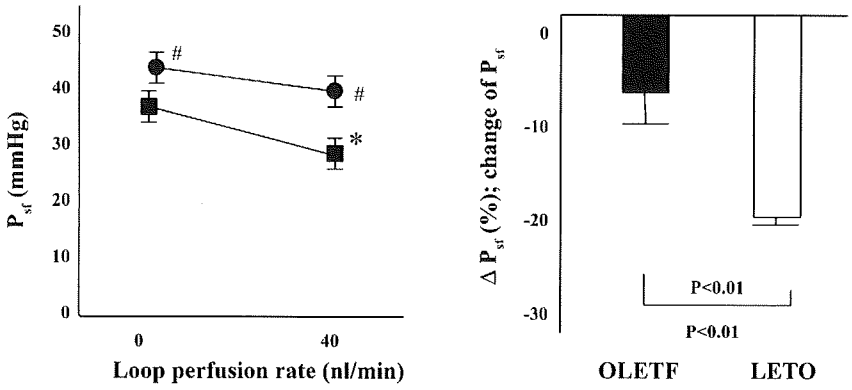

Fig. 8. P_{sf} and ΔP_{sf} in OLETF and LETO rats at 30 wk. *Left*: relationship between P_{sf} and rate of loop perfusion rate (0, 40 nl/min) with ATF in OLETF rats (●: n = 13) compared with those in LETO rats (■: n = 13). *Right*: %change of P_{sf} in OLETF rats (■: n = 13) compared with those in LETO rats (□: n = 13). $P < 0.05$ vs. P_{sf} at 0 nl/min (*) and vs. LETO (#).

Glomeruli in rats, including those of the Long-Evans strain, and in other mammals are usually not found on the kidney surface. Previous direct measurements of P_{gc} in diabetes have been performed in STZ-treated Munich-Wister rats in which surface glomeruli can be found with regularity (7). In the present study, we used the method of partial cortical ablation, first introduced by Aukland et al. (1), to access glomerular structures and to compare P_{gc} in surface and deep nephron in LETO and OLETF rats. We found that the bleeding was well controllable and that the tissue damage appeared to be relatively minor. We observed in these studies that P_{gc} was higher in deep cortical than surface glomeruli in both nondiabetic and diabetic animals. Furthermore, P_{gc} of OLETF rats at 30 wk of age exceeded that of control rats in both regions of the kidney. Using the same method, Iversen et al. (10) reported that the pressure in surface glomeruli of spontaneously hypertensive rats at 10 or 70 wk of age was higher in deep cortical than surface glomeruli. One of the causes of the raised P_{gc} may be the suppressed TGF mechanism that was found by micropuncture examination of superficial nephrons.

Pathological examination of both surface and deep cortex was performed in LETO and OLETF rats at 40 wk of age to determine whether the functional disorder was associated with structural abnormalities. The area of deep cortical glomeruli was larger than that of surface glomeruli in both groups of rats. Similar differences have also been reported in humans at an older age (23). Comparison between LETO and OLETF rats revealed no significant difference in the area of surface glomeruli. In contrast, deep cortical glomeruli of OLETF rats were significantly larger than those of LETO rats. Furthermore, increased glomerular disease in deep nephrons of OLETF rats is indicated by the sclerosis index. These observations correspond remarkably well with the rise of glomerular pressure found in this nephron population. Toyota et al. (24) recently observed increased variations of glomerular volumes in 26- to 27-wk-old OLETF rats without systematic regional differences using computer microtomography. Numerous previous reports have supported a causal connection between glomerular pressure and glomerular sclerosis. Periodic distension of mesangial cells in culture causes increased production of cellular matrix, and this effect is markedly enhanced by a high glucose concentration (4, 20).

In summary, our study reveals profound dysfunction of autoregulation and TGF that is associated with higher P_{gc} and augmented glomerular pathology in a type 2 model of diabetes. Hyperfiltration and renal hemodynamic abnormalities were found to precede the rise of serum glucose levels, consistent with the notion that an inefficient autoregulation may contribute to the development of diabetic renal disease.

ACKNOWLEDGMENTS

The technical assistant of Hiromi Hazawa is gratefully acknowledged.

GRANTS

This work was supported by Grant No. 17590814 from the Japan Society for the Promotion of Science.

REFERENCES

1. **Aukland K, Heyeraas Tonder K, Naess G.** Capillary pressure in deep and superficial glomeruli of the rat kidney. *Acta Physiol Scand* 101: 418–427, 1977.
2. **Bell TD, DiBona GF, Wang Y, Brands MW.** Mechanisms for renal blood flow control early in diabetes as revealed by chronic flow measurement and transfer function analysis. *J Am Soc Nephrol* 17: 2184–2192, 2006.
3. **Carmines PK, Ohishi K, Ikenaga H.** Functional impairment of renal afferent arteriolar voltage-gated calcium channels in rats with diabetes mellitus. *J Clin Invest* 98: 2564–2571, 1996.
4. **Cortes P, Zhao X, Riser BL, Narins RG.** Role of glomerular mechanical strain in the pathogenesis of diabetic nephropathy. *Kidney Int* 51: 57–68, 1997.
5. **Hashimoto Y, Ideura T, Yoshimura A, Koshikawa S.** Autoregulation of renal blood flow in streptozocin-induced diabetic rats. *Diabetes* 38: 1109–1113, 1989.

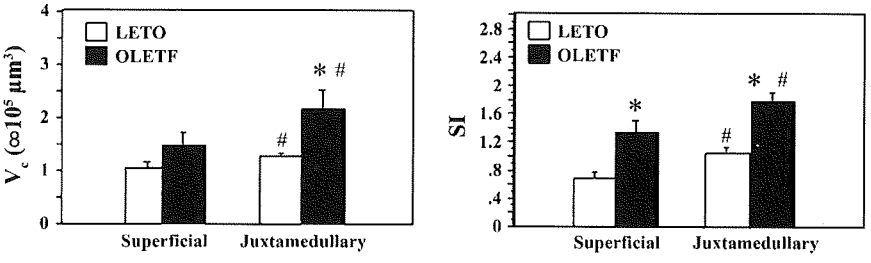

Fig. 9. Measurements of glomerular volume (V_G) and sclerosis index (SI) for both strains of rats at 30–40 wk.

6. **Hostetter TH, Rennke HG, Brenner BM.** The case for intrarenal hypertension in the initiation and progression of diabetic and other glomerulopathies. *Am J Med* 72: 375–380, 1982.
7. **Hostetter TH, Troy JL, Brenner BM.** Glomerular hemodynamics in experimental diabetes mellitus. *Kidney Int* 19: 410–415, 1981.
8. **Ikenaga H, Bast JP, Fallet RW, Carmines PK.** Exaggerated impact of ATP-sensitive K(+) channels on afferent arteriolar diameter in diabetes mellitus. *J Am Soc Nephrol* 11: 1199–1207, 2000.
9. **Ismail N, Becker B, Strzelczyk P, Ritz E.** Renal disease and hypertension in non-insulin-dependent diabetes mellitus. *Kidney Int* 55: 1–28, 1999.
10. **Iversen BM, Amann K, Kvam FI, Wang X, Ofstad J.** Increased glomerular capillary pressure and size mediate glomerulosclerosis in SHR juxtamedullary cortex. *Am J Physiol Renal Physiol* 274: F365–F373, 1998.
11. **Jamison RL.** Intrarenal heterogeneity. The case for two functionally dissimilar populations of nephrons in the mammalian kidney. *Am J Med* 54: 281–289, 1973.
12. **Kim S, Wanibuchi H, Hamaguchi A, Miura K, Yamanaka S, Iwao H.** Angiotensin blockade improves cardiac and renal complications of type II diabetic rats. *Hypertension* 30: 1054–1061, 1997.
13. **Koyama M, Wada R, Sakuraba H, Mizukami H, Yagihashi S.** Accelerated loss of islet beta cells in sucrose-fed Goto-Kakizaki rats, a genetic model of non-insulin-dependent diabetes mellitus. *Am J Pathol* 153: 537–545, 1998.
14. **Lewis EJ, Hunsicker LG, Clarke WR, Berl T, Pohl MA, Lewis JB, Ritz E, Atkins RC, Rohde R, Raz I.** Renoprotective effect of the angiotensin-receptor antagonist irbesartan in patients with nephropathy due to type 2 diabetes. *N Engl J Med* 345: 851–860, 2001.
15. **Majid DS, Navar LG.** Medullary blood flow responses to changes in arterial pressure in canine kidney. *Am J Physiol Renal Fluid Electrolyte Physiol* 270: F833–F838, 1996.
16. **Mattson DL, Lu S, Roman RJ, Cowley AW Jr.** Relationship between renal perfusion pressure and blood flow in different regions of the kidney. *Am J Physiol Regul Integr Comp Physiol* 264: R578–R583, 1993.
17. **Newbold KM, Sandison A, Howie AJ.** Comparison of size of juxtamedullary and outer cortical glomeruli in normal adult kidney. *Virchows Arch A Pathol Anat Histopathol* 420: 127–129, 1992.
18. **Okada M, Takemura T, Yanagida H, Yoshioka K.** Response of mesangial cells to low-density lipoprotein and angiotensin II in diabetic (OLETF) rats. *Kidney Int* 61: 113–124, 2002.
19. **Raij L, Azar S, Keane W.** Mesangial immune injury, hypertension, and progressive glomerular damage in Dahl rats. *Kidney Int* 26: 137–143, 1984.
20. **Riser BL, Cortes P, Zhao X, Bernstein J, Dumler F, Narins RG.** Intraglomerular pressure and mesangial stretching stimulate extracellular matrix formation in the rat. *J Clin Invest* 90: 1932–1943, 1992.
21. **Roald AB, Ofstad J, Iversen BM.** Attenuated buffering of renal perfusion pressure variation in juxtamedullary cortex in SHR. *Am J Physiol Renal Physiol* 282: F506–F511, 2002.
22. **Roman RJ, Zou AP.** Influence of the renal medullary circulation on the control of sodium excretion. *Am J Physiol Regul Integr Comp Physiol* 265: R963–R973, 1993.
23. **Samuel T, Hoy WE, Douglas-Denton R, Hughson MD, Bertram JF.** Determinants of glomerular volume in different cortical zones of the human kidney. *J Am Soc Nephrol* 16: 3102–3109, 2005.
24. **Toyota E, Ogasawara Y, Fujimoto K, Kajita T, Shigeto F, Asano T, Watanabe N, Kajiya F.** Global heterogeneity of glomerular volume distribution in early diabetic nephropathy. *Kidney Int* 66: 855–861, 2004.
25. **Uehara Y, Hirawa N, Numabe A, Kawabata Y, Nagoshi H, Negoro H, Fujiwara S, Gomi T, Ikeda T, Goto A, Omata M.** Angiotensin-converting enzyme inhibition delays onset of glucosuria with regression of renal injuries in genetic rat model of non-insulin-dependent diabetes mellitus. *J Cardiovasc Pharmacol Ther* 3: 327–336, 1998.
26. **Uriu K, Kaizu K, Qie YL, Kai K, Ito A, Ikeda M, Hashimoto O, Sun XF, Morita E, Eto S.** Renal hemodynamics in Otsuka Long-Evans Tokushima fatty rat, a model rat of spontaneous non-insulin-dependent diabetes mellitus with obesity. *J Lab Clin Med* 134: 483–491, 1999.
27. **Vallon V, Blantz RC, Thomson S.** Homeostatic efficiency of tubuloglomerular feedback is reduced in established diabetes mellitus in rats. *Am J Physiol Renal Fluid Electrolyte Physiol* 269: F876–F883, 1995.
28. **Vora JP, Zimsen SM, Houghton DC, Anderson S.** Evolution of metabolic and renal changes in the ZDF/Drt-fa rat model of type II diabetes. *J Am Soc Nephrol* 7: 113–117, 1996.
29. **Weibel ER.** Measuring through the microscope: development and evolution of stereological methods. *J Microsc* 155: 393–403, 1989.

Aberrant ENaC activation in Dahl salt-sensitive rats

Yutaka Kakizoe[a], Kenichiro Kitamura[a], Takehiro Ko[a], Naoki Wakida[a], Ai Maekawa[a], Taku Miyoshi[a], Naoki Shiraishi[a], Masataka Adachi[a], Zheng Zhang[b], Shyama Masilamani[b] and Kimio Tomita[a]

Background: The epithelial sodium channel (ENaC) plays an important role in the regulation of blood pressure by modulating Na reabsorption in the kidney. Dahl salt-sensitive rats on high-salt diet develop severe hypertension, and high-salt diet has been reported to stimulate ENaC mRNA expression in the kidney abnormally in Dahl salt-sensitive rats despite a suppressed plasma aldosterone concentration (PAC).

Methods: We investigated the effect of high-salt diet on ENaC protein expression in Dahl salt-resistant and Dahl salt-sensitive rats, and examined the effect of amiloride (5 mg/kg per day) and eplerenone (0.125% diet) on blood pressure and renal injury in Dahl salt-sensitive rats.

Results: Dahl salt-sensitive rats developed hypertension and renal damage following 4 weeks of treatment with high-salt diet. Although PAC and kidney aldosterone content were all suppressed by the high-salt diet in Dahl salt-sensitive rats, both β and γENaC mRNA expression and protein abundance were significantly increased. The molecular weight shift of γENaC from 85 to 70 kDa, an indication of ENaC activation, was clearly increased in Dahl salt-sensitive rats on high-salt diet compared with the low-salt group or Dahl salt-resistant rats on high-salt diet. Four weeks of treatment with amiloride, but not eplerenone, significantly ameliorated hypertension and kidney injury in Dahl salt-sensitive rats fed high-salt diet, suggesting aberrant aldosterone-independent activation of ENaC.

Conclusion: These results suggest that inappropriate expression and activation of ENaC could be one of the underlying mechanisms by which Dahl salt-sensitive rats develop salt-sensitive hypertension and organ damage, and indicate a therapeutic benefit of amiloride in salt-sensitive hypertension where ENaC is excessively activated.
J Hypertens 27:1679–1689 © 2009 Wolters Kluwer Health | Lippincott Williams & Wilkins.

Journal of Hypertension 2009, 27:1679–1689

Keywords: aldosterone, amiloride, eplerenone, Dahl salt-resistant and salt-sensitive hypertensive rat, epithelial sodium channel

Abbreviations: ANOVA, Analysis of variance; BP, blood pressure; BW, Body weight; Cr, creatinine; DR, Dahl salt-resistant rat; DS, Dahl salt-sensitive rat; ENaC, epithelial sodium channel; GAPDH, glyceraldehyde-3-phosphate dehydrogenase; HS, high-salt diet; HW, Heart weight; KW, Kidney weight; LS, low-salt diet; MCP-1, Monocyte chemotactic protein-1; PAC, plasma aldosterone concentration; PAS, Periodic acid-Schiff; PCR, Polymerase chain reaction; PRA, plasma renin activity; RAAS, renin–angiotensin–aldosterone system; RNA, Ribonucleic acid; SBP, systolic blood pressure; SDS-PAGE, Sodium dodecyl sulfate-polyacrylamide gel electrophoresis; TAL, thick ascending limb; TGF-1, Transforming growth facter-1; TP, Total protein

[a]Department of Nephrology, Kumamoto University Graduate School of Medical Sciences, Kumamoto, Japan and [b]Division of Nephrology, Department of Internal Medicine, Virginia Commonwealth University Medical Center, Richmond, Virginia, USA

Correspondence to Kenichiro Kitamura, MD, PhD, Department of Nephrology, Kumamoto University Graduate School of Medical Sciences, 1-1-1 Honjo, Kumamoto, Kumamoto 860-8556, Japan
Tel: +81 96 373 5164; fax: +81 96 366 8458;
e-mail: ken@gpo.kumamoto-u.ac.jp

Received 12 August 2008 **Revised** 26 February 2009
Accepted 3 April 2009

Introduction

The control of blood pressure (BP) and extracellular fluid volume primarily depends on renal regulation of sodium excretion. Among several sodium transporters and channels in the kidney, the epithelial sodium channel (ENaC) plays an important role in the regulation of BP by modulating sodium reabsorption in the distal nephron. ENaC consists of α, β, and γ subunits [1], and the activation of ENaC are mainly regulated by the rennin–angiotensin–aldosterone system (RAAS) [2,3]. As a result, patients with primary aldosteronism suffer from hypertension, hypokalemia and metabolic alkalosis. Also, mutations in ENaC cause disturbances of BP as observed in Liddle's syndrome [4,5] and pseudohypoaldosteronism type 1 [5].

In rats, aldosterone increases αENaC protein abundance and leads to the redistribution of its three subunits to the apical region of cortical collecting duct principal cells. In addition, aldosterone induces a molecular weight shift of γENaC from 85 to 70 kDa [3] and this shift is thought to be associated with activation of ENaC. The Dahl salt-sensitive hypertensive rat is an animal model for human salt-sensitive hypertension and it develops severe hypertension and organ damage with a high-salt diet [6]. Although the mechanisms by which Dahl salt-sensitive rats develop hypertension when fed high-salt diet are not fully understood, a previous study has reported that high-salt diet activated local RAAS (angiotensinogen, angiotensin II and aldosterone levels) in the heart and kidney from Dahl salt-sensitive rats in spite of suppressed plasma renin activity (PRA) and plasma aldosterone concentration (PAC) [7–9]. Supporting these reports, several studies showed that eplerenone, a selective aldosterone receptor blocker, had therapeutic effects on hypertension and heart and kidney injuries due to

0263-6352 © 2009 Wolters Kluwer Health | Lippincott Williams & Wilkins

DOI:10.1097/HJH.0b013e32832c7d23

high-salt diet in Dahl salt-sensitive rats [10–17]. An alternative possibility is that ENaC mRNA expression in the kidney from Dahl salt-sensitive rats was abnormally stimulated with high-salt diet despite lower PAC than with the low-salt diet [18,19]. In addition, injecting aldosterone into adrenalectomized Dahl salt-sensitive rats showed an increase in αENaC mRNA expression, but a decrease in β and γENaC [20]. These abnormalities in RAAS and ENaC expression in Dahl salt-sensitive rats could be responsible for the development of hypertension.

Amiloride has been used as a potassium-sparing diuretic that blocks sodium reabsorption through ENaC mainly in the distal segment of the kidney tubule [21–24]. It has potent antihypertensive effects especially in the states of ENaC activation such as Liddle's syndrome [21]. If the main cause of hypertension in Dahl salt-sensitive rats were activation of ENaC, amiloride would attenuate the elevated BP and organ damage. However, to our knowledge, there are no reports studying the effect of chronic oral administration of amiloride on Dahl salt-sensitive rats with high-salt diet. Therefore, in the current studies, we investigated the effect of high-salt diet on ENaC mRNA and protein expression in Dahl salt-resistant and Dahl salt-sensitive rats and examined the effect of amiloride and eplerenone on BP and kidney injury in Dahl salt-sensitive rats.

Materials and methods

Animals

All of the animal procedures were in accordance with the guidelines for care and use of laboratory animals approved by Kumamoto University. Eight week-old male Dahl salt-resistant and Dahl salt-sensitive rats were obtained from Kyudo Co., Ltd. (Saga, Japan). Rats were housed in a room maintained at constant temperature, humidity, and light cycle (12-h light/dark).

Protocol 1

The Dahl salt-sensitive rats ($n = 7$) were kept for 4 weeks under the following conditions: low-salt diet (0.3% NaCl), high-salt diet (8% NaCl) with free access to water and chow. The systolic blood pressure (SBP) was measured every week under awake conditions using a tail cuff method (MK-2000; Muromachi Kikai Co., Ltd., Osaka, Japan). Twenty-four hour urine collections were performed in metabolic cages every week, and urine protein was measured. After 4 weeks, rats were sacrificed under anesthetic conditions with pentobarbital sodium (50 mg/kg body weight). Heart and kidneys were weighed, and the left kidney was immediately frozen in the liquid nitrogen and stored at −80°C for measurement of kidney aldosterone content. The right kidney was sliced into approximately 3 mm thick sections and the cortex was separated from the medulla by sharp dissection. Blood samples were collected from the inferior vena cava and creatinine, electrolytes, total protein, PRA, and PAC were measured by commercial laboratory (SRL, Tokyo, Japan).

Protocol 2

The Dahl salt-resistant and Dahl salt-sensitive rats ($n = 7$) were kept for 4 weeks under the high-salt diet conditions with free access to water and chow. SBP measurement and 24 h urine collection were performed every week. After 4 weeks, rats were sacrificed, and kidneys and blood samples were obtained as described earlier.

Protocol 3

The Dahl salt-sensitive rats ($n = 6$) were kept for 4 weeks under low-salt diet, high-salt diet with vehicle (high-salt + V), eplerenone (0.125% in rodent chow, high-salt + E), or amiloride (5 mg/kg per day in drinking water, high-salt + A) with free access to water and chow. SBP measurement and 24 h urine collection were performed every 2 weeks. After 4 weeks, rats were sacrificed, and kidneys and blood samples were obtained as described earlier.

Immunoblotting

Pieces of kidney cortex were homogenized with the Polytron in ice-cold isolation solution containing 250 mmol/l sucrose/10 mmol/l trietanolamine (Sigma, St. Louis, Missouri, USA) with 1 μg/ml leupeptin (Sigma) and 0.1 mg/ml phenylmethyl sulfonyl floride (Sigma). Differential centrifugations were carried out to yield membrane fractions (17 000*g* and 200 000*g*). The 200 000*g* pellets were dissolved and protein concentration was determined by a bicinchoninic acid reaction (Pierce Biotechnology, Rockford, Illinois, USA). Aliquots of 30 μg proteins were subjected to SDS-PAGE, and immunoblotted with anti-ENaC, antiprostasin (BD Biosciences, San Jose, California, USA) and β-actin antibobies (Santa Cruz Biotechnology, Inc., Santa Cruz, California, USA). Antibodies to αENaC were a kind gift from Mark A. Knepper, previously characterized [3]. The antibodies to β and γENaC were developed in the Masilamani laboratory and our laboratory. The same method for antibody development and affinity purification was used as previously described [3]. Urine sample (ten-thousandth part of 24 h urine volume) from each rat was directly subjected to SDS-PAGE under reducing condition and analyzed by immunoblotting with antiprostasin antibody.

Real time reverse transcription polymerase chain reaction

A piece of kidney cortex was placed in RNAlater (Ambion Inc., Austin, Texas, USA) at 4°C overnight. Total RNA was extracted with TRIzol (Invitrogen, Carlsbad, California, USA) and RNeasy Micro Kit (Qiagen, Hilden, Germany). One microgram of total RNA was first transcribed with QuantiTect Reverse Transcription kit (Qiagen). TaqMan probes for rat ENaC α, β, and γ

subunits, collagen I, collagen III, TGF-β1, B7-1, MCP-1, and GAPDH were all purchased from Applied Biosystems (Foster City, California, USA). Real-time PCR was performed with an ABI PRISM 7900 Sequence Detector System (Applied Biosystems). Statistical analysis of results was performed with the ΔCt value ($Ct_{gene\ of\ interest}$-Ct_{GAPDH}). Relative gene expression was obtained by the ΔΔCt method (Ct_{sample}-$Ct_{calibrator}$).

Kidney histopathology

The kidneys were fixed with 4% paraformaldehyde and embedded in paraffin. Sections (2 μm thick) were stained with periodic acid-Schiff (PAS). The kidney sections were analyzed for degree of glomerulosclerosis, defined as disappearance of cellular elements from tuft, capillary loop collapse, and folding of the glomerular basement membrane with accumulation of amorphous material. The glomerulosclerosis score was calculated as described previously [25]. Approximately, 100 to 150 glomeruli were examined from each rat. Renal sections were scored in a blind manner.

Kidney aldosterone content

Left kidneys of Dahl salt-sensitive rats fed low-salt diet and high-salt diet were homogenized in ice-cold methanol (1 : 1.5 dilution, w/v), and centrifuged at 3000*g* for 15 min at 4°C. The supernatant was dried under nitrogen, and resuspended in an assay buffer for enzyme immunoassay kit (Cayman Chemical Corp., Ann Arbor, Michigan, USA).

Statistical analysis

Data are expressed as mean ± SD. Comparisons were made using the two-tailed, unpaired Student's *t*-test (protocol 1, 2) and ANOVA (protocol 3) followed by the Newman–Keuls method. $P < 0.05$ was considered as statistically significant.

Table 1 Body weight, organ weight, and blood parameters in Dahl salt-sensitive rats with low-salt and high-salt diet at 4 weeks

	LS	HS
BW (g)	380 ± 9	367 ± 14
HW/BW (mg/g)	3.2 ± 0.4	4.4 ± 0.3*
KW/BW (mg/g)	6.8 ± 0.3	9.3 ± 0.5*
Cr (mg/dl)	0.41 ± 0.04	0.37 ± 0.06
TP (mg/dl)	6.3 ± 0.1	5.8 ± 0.2†
Na (mEq/l)	144 ± 1	145 ± 1
K (mEq/l)	4.5 ± 0.1	3.9 ± 0.2*
PRA (ng/ml per h)	25.1 ± 13.2	2.6 ± 2.2†
PAC (pg/ml)	405 ± 166	147 ± 75†

Data are expressed as mean ± SD ($n = 7$). LS, low-salt diet; HS, high-salt diet; BW, body weight; Cr, creatinine; HW/BW, heart weight/body weight; KW/BW, kidney weight/body weight; PAC, plasma aldosterone concentration; PRA, plasma renin activity; TP, total protein. †$P < 0.01$ vs. LS. *$P < 0.001$ vs. LS.

Results

Protocol 1

Body weight, organ weight and blood pressure

Body weights (BW) in both groups were not different, but kidney weight/body weight (KW/BW) and heart weight/body weight (HW/BW) in the high-salt group were significantly increased compared with those in low-salt group (Table 1). SBP in both groups was below 130 mmHg at 0 week, but SBP in the high-salt group gradually increased and was significantly higher than that in the low-salt group after 1 week (Fig. 1a). These findings are compatible with previous reports.

Blood and urine parameters

Serum creatinine and Na values in each group were similar. Although PRA and PAC were markedly suppressed by the high-salt diet, serum K levels in the high-salt group were significantly decreased (Table 1). Urinary protein levels were dramatically increased in the high-salt group, suggesting severe kidney injury (Fig. 1b).

Fig. 1

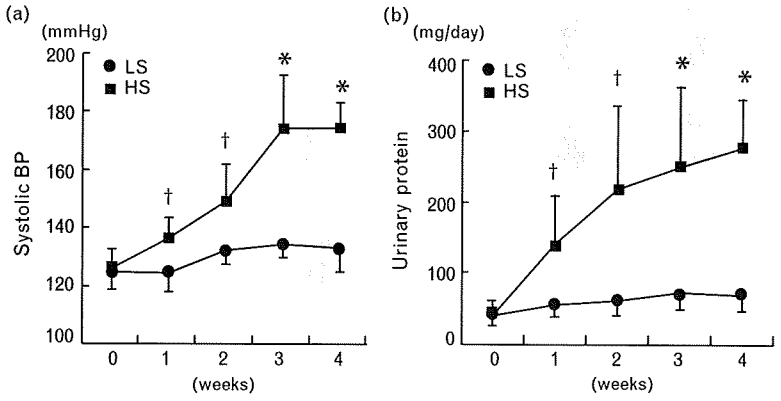

Effects of high-salt diet on SBP (a) and urinary protein (b) in Dahl salt-sensitive rats. SBP was measured by tail-cuff method weekly. Twenty-four hour urine collections were made in metabolic cages and urinary protein concentrations were determined at each time point. Data are expressed as mean ± SD ($n = 7$). LS; low-salt diet, and HS; high-salt diet. †$P < 0.01$ vs. LS, and *$P < 0.001$ vs. LS.

Correspondently, high-salt diet decreased serum total protein levels in Dahl salt-sensitive rats (Table 1).

mRNA and protein expression of ENaC in the kidney

Expression levels of αENaC mRNA in the kidney were almost identical in both groups. On the contrary, both β and γENaC mRNA were significantly increased in high-salt group compared with low-salt group (1.46 ± 0.31 and 1.50 ± 0.13 fold increase over low-salt group, respectively) (Fig. 2a). Protein abundances of αENaC were almost equal in both groups, but βENaC and 85 kDa form of γENaC was significantly increased by the high-salt diet (2.05 ± 0.04 and 1.47 ± 0.10 fold increase over low-salt group, respectively) (Fig. 2b). This result of protein abundances matched mRNA expression. Surprisingly, the 70 kDa form of γENaC, usually detected under conditions with elevated circulating aldosterone levels, was obviously increased in high-salt group rather than in low-salt group despite suppressed plasma aldosterone levels (1.77 ± 0.35 fold increase over low-salt group, respectively) (Fig. 2b).

Protocol 2

Blood pressure, blood and urine parameters

At 0 week, SBP and the amount of urinary protein were slightly higher in Dahl salt-sensitive rats than in Dahl salt-resistant rats. The high-salt diet did not affect SBP and urinary protein in Dahl salt-resistant rats, but it significantly increased those in Dahl salt-sensitive rats as rats grew up (Fig. 3). Serum Na values in each group were similar. Although PACs of both strains were almost same levels on high-salt diet, serum K levels in Dahl salt-sensitive rats were significantly lower than those in Dahl salt-resistant rats (Table 2).

mRNA and protein expression of ENaC in the kidney

The mRNA and protein expressions of αENaC in the kidney were almost comparable levels in both strains under high-salt diet (Fig. 4). Both β and γENaC mRNA

Fig. 2

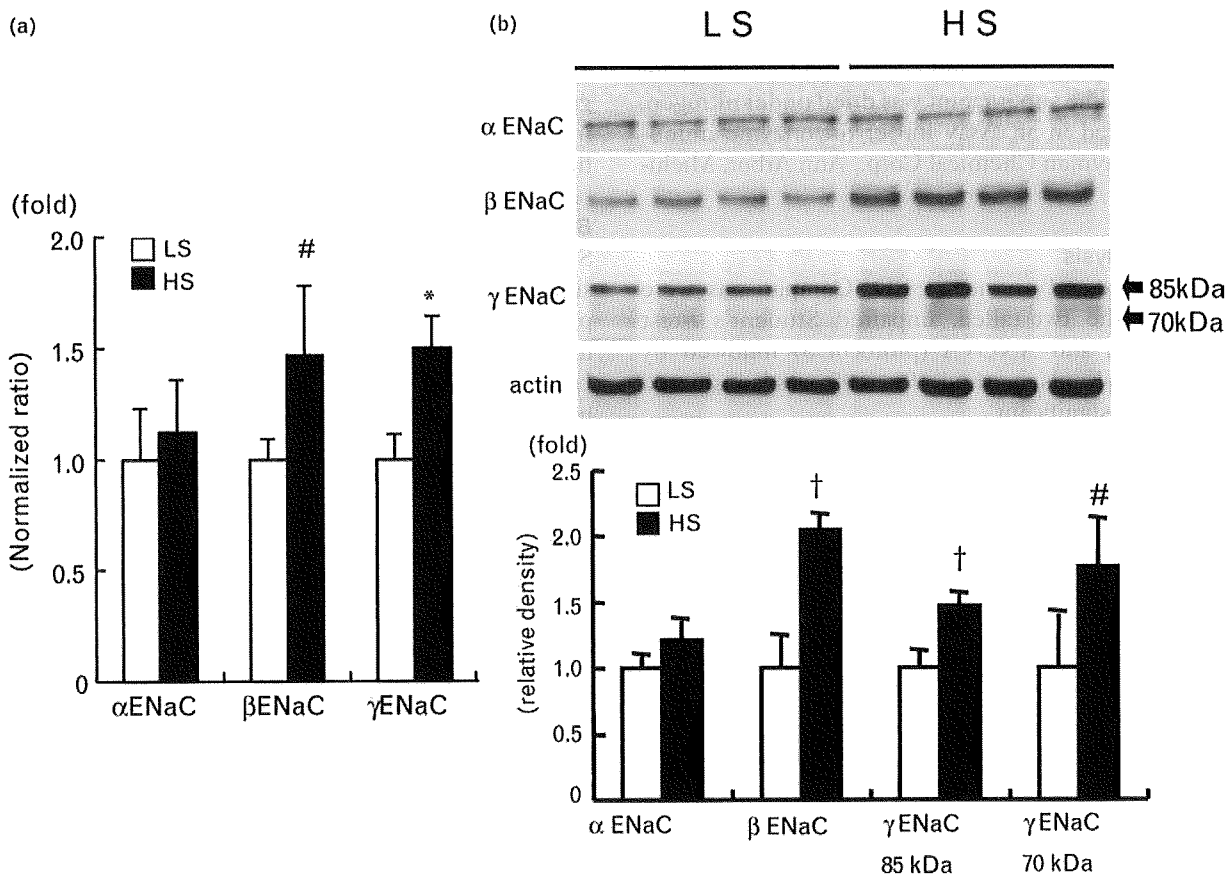

Effects of high-salt diet on mRNA (a) and protein (b) expression of ENaC subunits in the kidney cortex from Dahl salt-sensitive rats at 4 weeks. (a) mRNA expression of ENaC subunits was determined by real-time PCR. The abundance of each mRNA was normalized for GAPDH. (b) Protein expressions of ENaC subunits and β-actin were evaluated by western blot analysis (upper panel). The densitometry values are normalized for β-actin. Values are expressed as fold increase over low-salt diet and summarized in the bar graph (lower panel). Data are expressed as mean ± SD ($n = 7$). LS; low-salt diet, and HS; high-salt diet. $^{\#}P < 0.05$ vs. LS, $^{\dagger}P < 0.01$ vs. LS, and $^{*}P < 0.001$ vs. LS.

Fig. 3

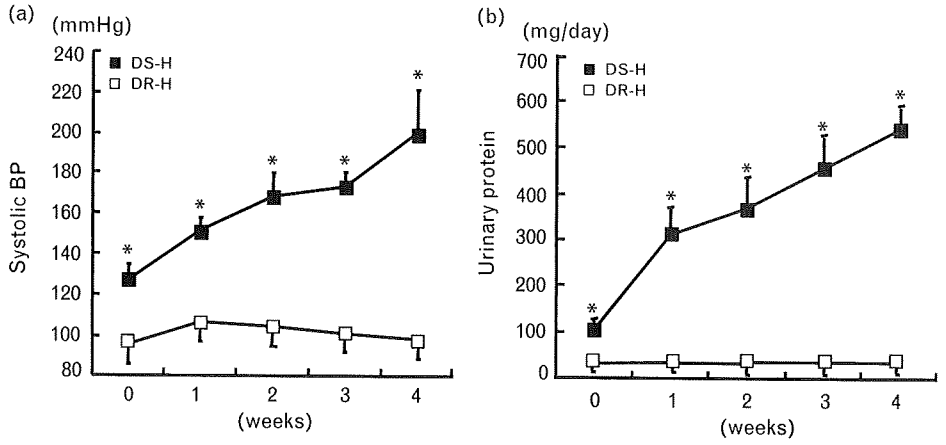

Effects of high-salt diet on SBP (a) and urinary protein (b) in Dahl salt-resistant and Dahl salt-sensitive rats. SBP was measured by tail-cuff method weekly. Twenty-four hour urine collections were made in metabolic cages and urinary protein concentrations were determined at each time point. Data are expressed as mean ± SD ($n = 7$). DR-H; Dahl salt-resistant rats with high-salt diet. DS-H; Dahl salt-sensitive rats with high-salt diet. *$P < 0.001$ vs. DR-H.

were significantly increased in Dahl salt-sensitive rats compared with Dahl salt-resistant rats (1.17 ± 0.07 and 1.14 ± 0.08 fold increase over Dahl salt-resistant rats, respectively) (Fig. 4a). Both of βENaC and 85 kDa form of γENaC were more abundant in Dahl salt-sensitive rats (1.56 ± 0.15 and 1.36 ± 0.14 fold increase over Dahl salt-resistant rats, respectively) (Fig. 4b). Furthermore, the 70 kDa form of γENaC was apparently increased in Dahl salt-sensitive rats despite the similar PAC levels (1.90 ± 0.20 fold increase over Dahl salt-resistant rats, respectively) (Fig. 4b).

Kidney and urinary prostasin

To elucidate the mechanisms by which Dahl salt-sensitive rats increase the 70 kDa form of γENaC under high-salt diet, we examined the protein abundance of prostasin, which is one of the serine proteases that cleaves γENaC, in the kidney and urine. Kidney prostasin abundance in Dahl salt-sensitive rats on high-salt diet was not different from those in Dahl salt-sensitive rats on low-salt diet or Dahl salt-resistant rats on high-salt diet (Fig. 5a). The 4 weeks treatment of high-salt diet significantly increased urine prostasin in Dahl salt-sensitive rats (Fig. 5b).

Table 2 Blood parameters in Dahl salt-resistant and Dahl salt-sensitive rats with high-salt diet at 4 weeks

	DR-H	DS-H
Na (mEq/l)	144 ± 1	145 ± 1
K (mEq/l)	4.4 ± 0.5	3.8 ± 0.2#
PRA (ng/ml per h)	5.6 ± 2.5	3.2 ± 1.5#
PAC (pg/ml)	185 ± 67	185 ± 25

Data are expressed as mean ± SD ($n = 7$). DR-H, Dahl salt-resistent rats with high-salt diet; DS-H, Dahl salt-sensitive rats with high-salt diet; PAC, plasma aldosterone concentration; PRA, plasma renin activity. # $P < 0.05$ vs. DR-H.

Protocol 3

Body weight, organ weight and blood pressure

Amiloride significantly reduced KW/BW and HW/BW in Dahl salt-sensitive rats fed with high-salt diet whereas eplerenone had no effect (Table 3). The SBP was almost comparable among three groups with high-salt diet at 2 weeks (Fig. 6a). At 4 weeks, the SBP in high-salt + V group was increased to over 170 mmHg, whereas treatment with amiloride but not eplerenone significantly attenuated high-salt diet-induced hypertension in Dahl salt-sensitive rats (Fig. 6a).

Blood and urine parameters

The differences of blood and urine parameters in low-salt group and high-salt + V group were almost same as in protocol 1. Serum Na was reduced and serum K, PRA, and PAC levels were all increased in the high-salt + A group compared to the high-salt + V group, indicating that amiloride blocked sodium reabsorption through ENaC in the kidney (Table 3). Although eplerenone increased serum K and PRA, we did not find any increase in PAC levels compared with the high-salt + V group. Treatment with amiloride but not eplerenone substantially improved proteinuria caused by high-salt diet at 4 weeks (Fig. 6b).

Kidney injury (expression of collagen, TGF-β1, B7-1, and MCP-1 genes)

Since amiloride exhibited antihypertensive and renoprotective effects in Dahl salt-sensitive rats with high-salt diet, we evaluated changes in the mRNA expression levels of renal injury markers by real-time PCR. Collagen type I, type III, TGF-β1, B7-1, and MCP-1 mRNA levels were significantly increased in high-salt + V group

Fig. 4

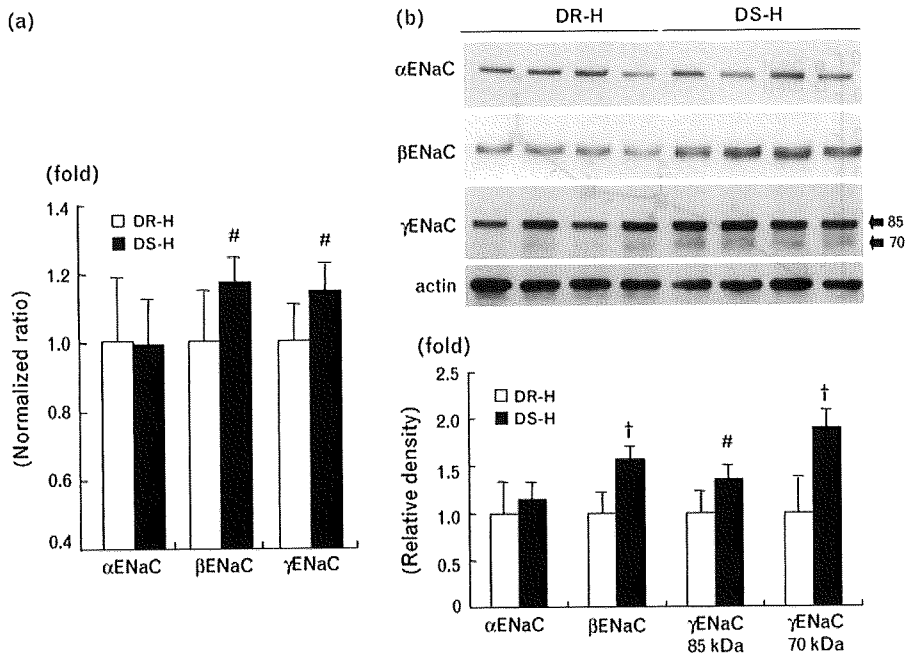

Effects of high-salt diet on mRNA (a) and protein (b) expression of ENaC subunits in the kidney cortex from Dahl salt-resistant and Dahl salt-sensitive rats at 4 weeks. (a) mRNA expression of ENaC subunits was determined by real-time PCR. The abundance of each mRNA was normalized for GAPDH. (b) Protein expressions of ENaC subunits and β-actin were evaluated by western blot analysis (upper panel). The densitometry values are normalized for β-actin. Values are expressed as fold increase over Dahl salt-resistant rats with high-salt diet and summarized in the bar graph (lower panel). Data are expressed as mean ± SD ($n = 7$). DR-H; Dahl salt-resistant rats with high-salt diet. DS-H; Dahl salt-sensitive rats with high-salt diet. $^{\#}P < 0.05$ vs. DR-H, and $^{\dagger}P < 0.01$ vs. DR-H.

compared with low-salt group (1.84 ± 0.27, 1.85 ± 0.31, 1.54 ± 0.22, 2.09 ± 0.39, and 1.77 ± 0.81 fold increase over low-salt group, respectively) (Fig. 7). When compared with the high-salt + V group, the high-salt + A group demonstrated a significant decrease in all kidney injury markers mRNA levels (Fig. 7). However, treatment with eplerenone did not show a beneficial effect on kidney injury (Fig. 7).

Kidney histopathology

Light microscopic examination of PAS-stained renal sections showed that some glomeruli suffered fibrinoid necrosis in the capillary tuft with increased PAS-positive materials, cellular proliferation, and sclerosis in high-salt + V group. In addition, atrophic and dilated tubules with tubular cast were observed in high-salt + V group. These changes were obviously reduced in high-salt + A group, but not in high-salt + E group (Fig. 8a). The glomerulosclerosis score was significantly increased in high-salt + V group compared with low-salt group. The glomerulosclerosis induced by high-salt diet was clearly ameliorated by treatment with amiloride (Fig. 8b).

Kidney aldosterone content

In the current study, we could not observe either antihypertensive or renoprotective effects of eplerenone on Dahl salt-sensitive rats in contrast to previous reports by other investigators [10,12,13,16]. Since the organ protective effect of eplerenone is expected presumably based on the finding that the local RAAS is activated by the high-salt diet despite suppression of systemic RAAS, we determined tissue aldosterone content in the kidneys from Dahl salt-sensitive rats in protocol 1. Kidney aldosterone content was markedly suppressed by the high-salt diet compared with the low-salt diet (low-salt: 392 ± 91 pg/ml vs. high-salt: 136 ± 69 pg/ml, $P < 0.01$). These values were almost in parallel with systemic aldosterone levels. In our hands, the local RAAS in the kidney was not activated by high-salt diet in Dahl salt-sensitive rats.

Discussion

In the present studies, we first investigated the effect of high-salt diet on ENaC mRNA and protein expression in the kidneys of Dahl salt-sensitive rats. Although PRA, PAC as well as kidney aldosterone content were all suppressed by the high-salt diet, the mRNA expression of αENaC in the high-salt group was comparable to that of the low-salt group and both β and γENaC were significantly increased in high-salt group. Previously Aoi *et al.* [19] reported that high-salt diet increased the mRNA expression of all ENaC subunits, whereas our

Fig. 5

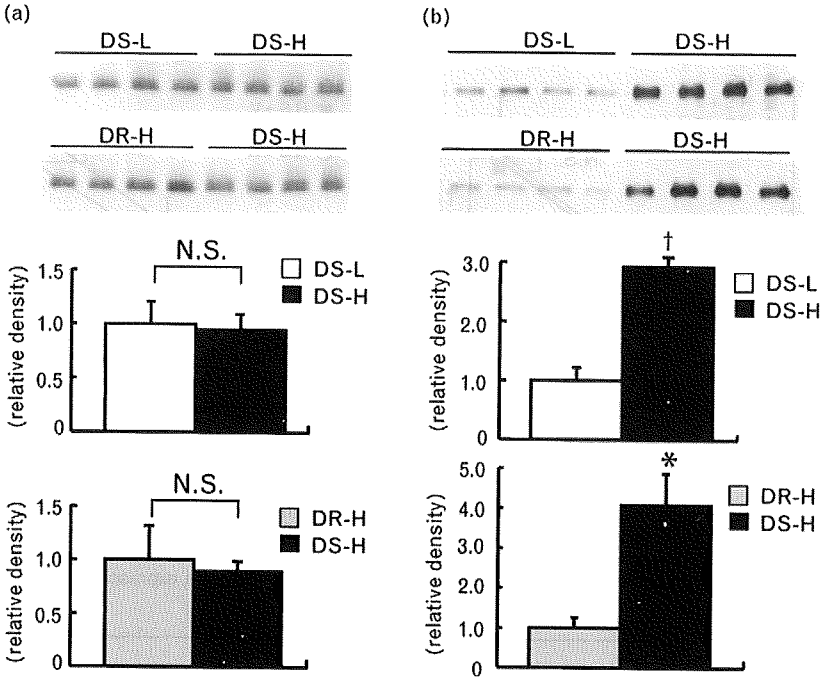

Immunoblotting of kidney and urinary prostasin. Protein expressions of prostasin in the kidney (a) or in the urine (b) were evaluated by western blot analysis. The densitometry values are normalized for β-actin (a) or urine volumes per day (b) as described in the methods section. Values are expressed as fold increase over DS-L (a; upper panel), DR-H (a; lower panel), DS-L (b; upper panel), or DR-H (b; lower panel). Data are expressed as mean ± SD ($n = 7$). DS-L; Dahl salt-sensitive rats with low-salt diet. DS-H; Dahl salt-sensitive rats with high-salt diet. DR-H; Dahl salt-resistant rats with high-salt diet. NS, not significant. $^{\dagger}P < 0.01$ vs. DS-L. $^{*}P < 0.01$ vs. DR-H.

study demonstrated no significant change in α subunit mRNA. The reason for this discrepancy is not clear at this point. The only difference we could find was that the body weight of the high-salt group was significantly smaller than that of the low-salt group in their study [18,19]. We did not see any significant differences in body weights of Dahl salt-sensitive rats between the high-salt and low-salt groups in our hands. Further investigation will be required to determine if the changes in the body weight accounts for the differences in the αENaC expression. They also reported that subcutaneous injection of aldosterone into adrenalectomized Dahl salt-sensitive rats decreased the mRNA expression of β and γ subunits and increased α subunit expression [20], suggesting that the regulation of β and γENaC mRNA expression by aldosterone would be abnormal. Our current results revealed that Dahl salt-sensitive rats fed high-salt diet showed significantly lower serum potassium levels than Dahl salt-sensitive rats on low-salt diet even though PAC levels were markedly decreased in Dahl salt-sensitive rats on high-salt diet. Furthermore, Dahl salt-sensitive rats also have significantly lower serum potassium levels than Dahl salt-resistant rats under high-salt diet although PAC levels were almost equally suppressed in both strains. This aldosterone-independent suppression of serum potassium levels strongly suggests the possibility that ENaC is aberrantly activated in Dahl salt-sensitive rats even under high-salt diet. Why are these inappropriate regulations of ENaC provoked by high-salt diet in Dahl salt-sensitive rats? There were several studies investigating the differences in ENaC genes between Dahl salt-resistant and Dahl salt-sensitive rats [26–28]. However, none of them could see the differences in sequences of ENaC where they studied in Dahl salt-resistant and Dahl salt-sensitive rats. Therefore, we could not explain our results by the genetic differences in ENaC genes between Dahl salt-resistant and Dahl salt-sensitive rats.

Table 3 Effects of eplerenone and amiloride on body weight, organ weight, and blood parameters in Dahl salt-sensitive rats with high-salt diet at 4 weeks

	LS	HS + V	HS + E	HS + A
BW (g)	383 ± 7	375 ± 3	372 ± 13	373 ± 9
HW/BW (mg/g)	3.0 ± 0.4	4.6 ± 0.2†	4.4 ± 0.1†	4.0 ± 0.1†,§
KW/BW (mg/g)	6.7 ± 0.3	9.5 ± 0.4†	9.7 ± 0.7†	8.5 ± 0.5†,§
Cr (mg/dl)	0.41 ± 0.05	0.36 ± 0.06	0.39 ± 0.03	0.39 ± 0.05
TP (mg/dl)	6.3 ± 0.1	5.8 ± 0.2†	5.9 ± 0.2†	6.3 ± 0.1*
Na (mEq/l)	144 ± 1	144 ± 2	145 ± 1	142 ± 1§
K (mEq/l)	4.5 ± 0.2	3.9 ± 0.1†	4.6 ± 0.2*	5.3 ± 0.2†,*
PRA (ng/ml per h)	27.3 ± 17.9	1.9 ± 0.9†	5.2 ± 1.6$^{\#,\S}$	8.5 ± 1.2$^{\#,*}$
PAC (pg/ml)	425 ± 209	134 ± 90$^{\#}$	136 ± 39$^{\#}$	454 ± 221*

Data are expressed as mean ± SD ($n = 6$). BW, body weight; Cr, creatinine; HS + A, high-salt diet + amiloride; HS + E, high-salt diet + eplerenone; HS + V, high-salt diet + vehicle; HW/BW, heart weight/body weight; KW/BW, kidney weight/body weight; LS, low-salt diet; PAC, plasma aldosterone concentration; PRA, plasma renin activity; TP, total protein. $^{\#}P < 0.05$ vs. LS. $^{\dagger}P < 0.01$ vs. LS. $^{\S}P < 0.05$ vs. HS + V. $^{*}P < 0.01$ vs. HS + V.

Fig. 6

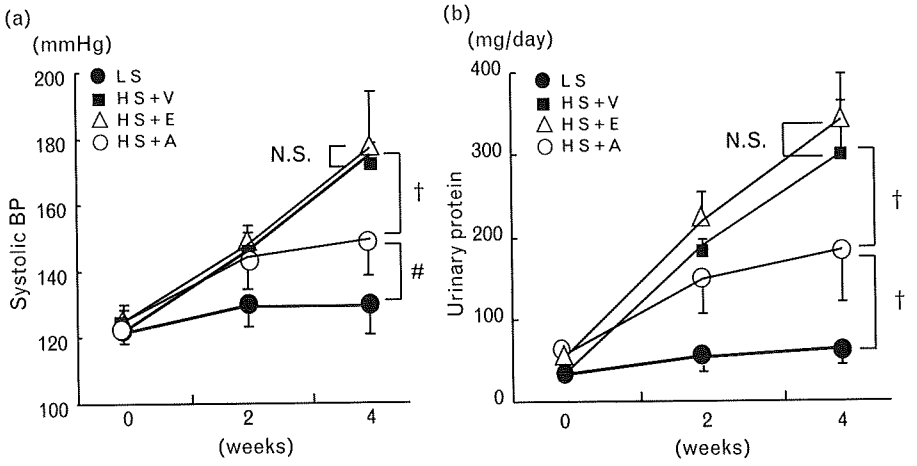

Effects of eplerenone and amiloride on hypertension and proteinuria in Dahl salt-sensitive rats with high-salt diet. Dahl salt-sensitive rats were fed low-salt (LS) and high-salt diets following eplerenone (0.125% in rodent chow, HS + E), amiloride (5 mg/kg per day in drinking water, HS + A) or vehicle (HS + V) treatment, and SBP was measured by tail-cuff method every 2 weeks. Twenty-four hour urine collections were made in the metabolic cages and urinary protein concentrations were determined at each time point. Data are expressed as mean ± SD ($n = 6$). NS, not significant. $^{\#}P < 0.05$. $^{\dagger}P < 0.01$.

Recently, Yasuhara *et al.* [29] demonstrated that high-salt diet increases transcriptional activity of collectrin in Wistar-Kyoto rats and spontaneously hypertensive rats that is independent of aldosterone action. They suggested that upregulation of collectrin by high-salt diet may be responsible for the sodium retention in salt-sensitive hypertension. Although they did not elucidate the precise signaling pathway, a similar signaling mechanism might be involved in the high-salt diet-induced increase in the mRNA expression in β and γENaC in Dahl salt-sensitive rats.

Here we show for the first time the regulation of ENaC at the protein level in Dahl salt-sensitive rats with a high-salt diet. Protein abundance of βENaC and 85 kDa form of γENaC was significantly increased by the high-salt diet, and also the molecular weight shift of γ subunit from 85 to

Fig. 7

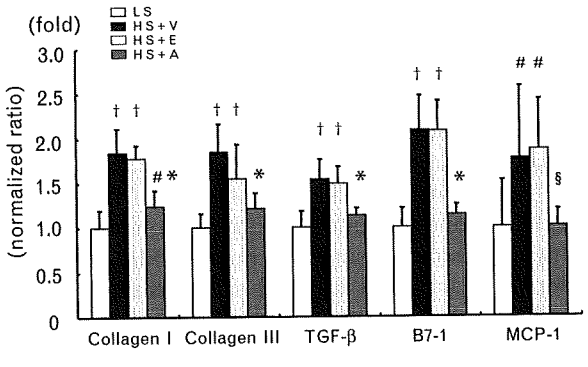

Effects of eplerenone and amiloride on kidney injury markers in Dahl salt-sensitive rats with high-salt diet at 4 weeks. mRNA expression of kidney injury makers was evaluated by real-time PCR following 4 weeks treatment of low-salt (LS) and high-salt diets with eplerenone (0.125% in rodent chow, HS + E), amiloride (5 mg/kg per day in drinking water, HS + A), or vehicle (HS + V). Abundance of each mRNA was normalized for GAPDH and values are expressed as fold increase over LS treatment. Data are expressed as mean ± SD ($n = 6$). $^{\#}P < 0.05$ vs. LS. $^{\dagger}P < 0.01$ vs. LS. $^{\S}P < 0.05$ vs. HS + V. $^{*}P < 0.01$ vs. HS + V.

Fig. 8

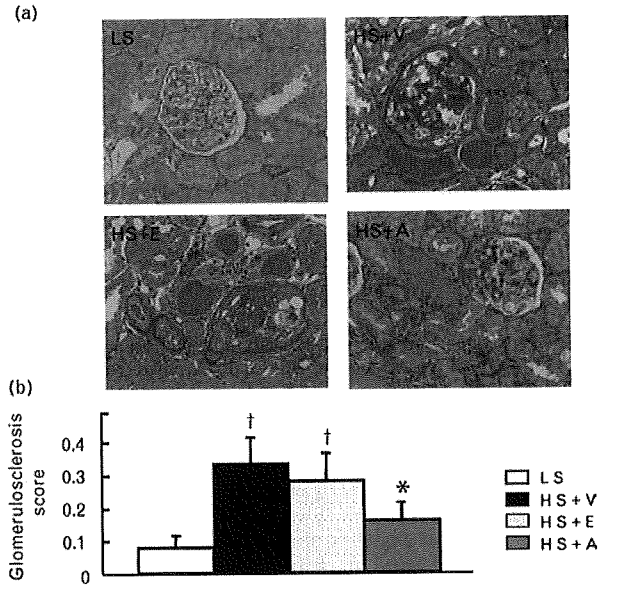

Effects of eplerenone and amiloride on kidney histopathology in Dahl salt-sensitive rats with high-salt diet at 4 weeks. (a) Representative photomicrographs (200×) of periodic acid-Schiff-stained kidney sections from Dahl salt-sensitive rats on low-salt diet (LS), those on high-salt diet with vehicle (HS + V), eplerenone (0.125% in rodent chow, HS + E) or amiloride (5 mg/kg per day in drinking water, HS + A). (E) Glomerulosclerosis score. Data are expressed as mean ± SD ($n = 6$). $^{\dagger}P < 0.01$ vs. LS. $^{*}P < 0.01$ vs. HS + V.

70 kDa was increased despite the suppression of plasma and kidney aldosterone concentrations. This molecular weight shift was first described by Masilamani *et al.* in 1999 [3]. They demonstrated that salt restriction or aldosterone infusion in rats resulted in a molecular weight shift of the ENaC γ subunit from 85 to 70 kDa. Since then, proteolytic modification of ENaC has been extensively studied. A series of studies from Kleyman's laboratory clearly demonstrated that proteolytic processing of α and γENaC is required for the activation of this channel. A serine protease furin cleaves the α subunit at two sites, releasing an inhibitory tract located in the extracellular loop of the α subunit and activating the channel [30,31]. On the contrary, furin cleaves the γ subunit only at one site. A second distal cleavage in the γ subunit induced by other proteases such as prostasin [32] and plasmin [33] is required to release another inhibitory tract located in the extracellular loop of the γ subunit and further activate the channel. The cleavage of the γENaC is now believed to be more important than αENaC [34]. In the current studies, we found that the shift of γENaC was more abundant in Dahl salt-sensitive rats fed high-salt diet than in those fed low-salt diet or Dahl salt-resistant rats fed high-salt diet despite lower or similar PAC. In addition, we demonstrated that urinary prostasin was more abundant in Dahl salt-sensitive rats fed high-salt diet than in those fed low-salt diet or Dahl salt-resistant rats fed high-salt diet. Since kidney prostasin proteins among these groups were not significantly different, the differences in urinary prostasin might be derived from those filtered through glomeruli considering the existence of prostasin in serum [35]. Since Dahl salt-sensitive rats on high-salt diet develop severe nephrotic syndrome, urinary prostasin filtered through glomuruli might cleave γENaC independent of PAC or kidney aldosterone content, leading to more severe hypertension. Svenningsen *et al.* [36] reported that urinary plasmin from nephrotic rats and humans activated ENaC, supporting our idea that urinary prostasin derived from serum is involved in the activation of ENaC. Recently, we reported that camostat mesilate (FOY-305), a synthetic serine protease inhibitor, markedly attenuated hypertension and kidney injury in Dahl salt-sensitive rats with high-salt diet [37]. These findings also indicate the importance of γENaC in the pathogenesis of salt-sensitive hypertension in Dahl salt-sensitive rats because camostat inhibits prostasin [37] and plasmin [38] but not furin [39].

In protocol 3, we investigated the effects of amiloride and eplerenone on Dahl salt-sensitive rats with high-salt diet in order to confirm the contribution of aldosterone-independent aberrant ENaC activation in the development of salt-sensitive hypertension. Amiloride significantly ameliorated hypertension and organ damage caused by the high-salt diet. Dahl salt-sensitive rats treated with amiloride showed decreased serum sodium levels, increased serum potassium levels, and increased PAC, indicating that amiloride effectively suppressed ENaC activity in the kidney and hence reduced the BP. Does this organ saving effect of amiloride depend on the antihypertensive effect? In previous animal studies where amiloride and salt were given to deoxycorticosterone acetate treated rats and stroke-prone spontaneously hypertensive rats, amiloride improved cardiac fibrosis and decreased urinary protein excretion despite the facts that it did not decrease BP, affect serum potassium levels, or urinary electrolytes [40,41]. Additionally, where amiloride was given to uninephrectomized aldosterone-salt treated rat, it lowered elevated BP and attenuated myocardical fibrosis not only in left but also in right ventricle. Considering the improvement of non-hypertensive right ventricles, the benefits of amiloride should not be derived only from the antihypertensive effect [42]. These findings indicate beneficial effects independent of the BP-lowering effects of amiloride on the salt-sensitive hypertension. However, in the current studies, we have not addressed the question whether the beneficial effects of amiloride are independent of the BP-lowering effects on the high-salt diet-induced kidney injury. PAC in amiloride treated Dahl salt-sensitive rats was about three-fold higher than those in vehicle or eplerenone-treated rats, suggesting the significant compensatory mineralocorticoid receptor activation in these rats compared with eplerenone treated rats. Nevertheless only amiloride had blood pressure lowering and renoprotective effects against high-salt diet, indicating that there are some cases in which drugs blocking ENaC would be more effective than mineralocorticoid receptor antagonists. O'Connor *et al.* [43] reported that amiloride reduced superoxide production in medullary thick ascending limb (TAL) cells of Dahl salt-sensitive rats independently of sodium transport. They showed that an increase in extracellular osmolarity not only by increment of superfusate NaCl concentration but by choline chloride concentration invoked cell shrinkage leading to activation of NHE and thereafter NADPH oxidase, and that amiloride reduced NADPH oxidase activation and superoxide production probably by blocking NHE. Therefore, it is possible that the antioxidant effect of amiloride independent of sodium transport would attenuate hypertension and kidney injury. On the contrary, Hong *et al.* [44] reported that furosemide but not amiloride decreased superoxide productions in TALs of Sprague–Dawley rats. They speculated that NaCl reabsorption through Na-K-2Cl cotransporter contribute to the generation of superoxide. Accordingly, it is still controversial whether superoxide production in TALs is independent of sodium transport and whether amiloride reduces superoxide production in TALs by blocking NHE.

Several studies demonstrated beneficial effects of eplerenone on Dahl salt-sensitive rats [10–17]. The rationale for these effects is based on the finding that the local RAAS is up regulated by high-salt diet in spite of suppression of the systemic RAAS. A previous report showed that a high-salt diet increased kidney aldosterone content in Dahl salt-sensitive rats [9]. However,

in our study, the high-salt diet suppressed kidney aldosterone content in parallel with PAC. In addition, we did not observe induction of mineralocorticoid receptors by the high-salt diet in the kidney (data not shown). This might be one reason why we did not see either antihypertensive or organ protective effects of eplerenone. At this point, we do not have an explanation for the differences in the therapeutic effects of eplerenone between the previous studies and ours. It may depend on the differences in the experimental protocols such as the timing of salt and drug administration or the age of the rats used for the studies. For example, Nagase *et al.* [13] started treating Dahl salt-sensitive rats with eplerenone 5 days before salt loading and high-salt diet was initiated at the age of 4 weeks. They showed a significant organ protective effect of eplerenone, whereas we initiated the drug and salt together at the age of 8 weeks and did not see an antihypertensive effect. Earlier treatment might result in better outcome in Dahl salt-sensitive rats.

In summary, in the present studies we demonstrated that both β and γENaC mRNA expression and protein abundance were significantly increased in Dahl salt-sensitive rats fed high-salt diet compared with Dahl salt-sensitive rats on low-salt diet or Dahl salt-resistant rats on high-salt diet. This abnormal expression and activation of ENaC could be one of the underlying mechanisms by which Dahl salt-sensitive rats develop salt-sensitive hypertension and organ damage. Our current data suggest a significant therapeutic effect of amiloride in salt-sensitive hypertension where ENaC is excessively activated.

Acknowledgements

The authors thank Dr R. Tyler Miller (Case Western Reserve University) for the critical reading of the manuscript and helpful discussion.

This work was supported by the following: Grants-in-Aid for Scientific Research from the Ministry of Education, Culture, Sports, Science and Technology in Japan (grant number 19590956 to K.K., 19590958 to T.M., 18790570 to N.S., 18790569 to M.A., and 18390252 to K.T.); Salt Science Research Foundation Grant (0728 to K.K.); Mitsubishi Pharma Research Foundation Grant (to K.K.); and Suzuken Memorial Foundation Grant (to K.K.).

References

1 Canessa CM, Schild L, Buell G, Thorens B, Gautschi I, Horisberger JD, *et al.* Amiloride-sensitive epithelial Na+ channel is made of three homologous subunits. *Nature* 1994; **367**:463–467.
2 Loffing J, Zecevic M, Feraille E, Kaissling B, Asher C, Rossier BC, *et al.* Aldosterone induces rapid apical translocation of ENaC in early portion of renal collecting system: possible role of SGK. *Am J Physiol Renal Physiol* 2001; **280**:F675–F682.
3 Masilamani S, Kim GH, Mitchell C, Wade JB, Knepper MA. Aldosterone-mediated regulation of ENaC alpha, beta, and gamma subunit proteins in rat kidney. *J Clin Invest* 1999; **104**:R19–R23.
4 Hansson JH, Schild L, Lu Y, Wilson TA, Gautschi I, Shimkets R, *et al.* A de novo missense mutation of the beta subunit of the epithelial sodium channel causes hypertension and Liddle syndrome, identifying a proline-rich segment critical for regulation of channel activity. *Proc Natl Acad Sci U S A* 1995; **92**:11495–11499.
5 Oh YS, Warnock DG. Disorders of the epithelial Na(+) channel in Liddle's syndrome and autosomal recessive pseudohypoaldosteronism type 1. *Exp Nephrol* 2000; **8**:320–325.
6 Rapp JP. Dahl salt-susceptible and salt-resistant rats. A review. *Hypertension* 1982; **4**:753–763.
7 Kobori H, Nishiyama A, Abe Y, Navar LG. Enhancement of intrarenal angiotensinogen in Dahl salt-sensitive rats on high salt diet. *Hypertension* 2003; **41**:592–597.
8 Kobori H, Nishiyama A. Effects of tempol on renal angiotensinogen production in Dahl salt-sensitive rats. *Biochem Biophys Res Commun* 2004; **315**:746–750.
9 Bayorh MA, Ganafa AA, Emmett N, Socci RR, Eatman D, Fridie IL. Alterations in aldosterone and angiotensin II levels in salt-induced hypertension. *Clin Exp Hypertens* 2005; **27**:355–367.
10 Bayorh MA, Mann G, Walton M, Eatman D. Effects of enalapril, tempol, and eplerenone on salt-induced hypertension in Dahl salt-sensitive rats. *Clin Exp Hypertens* 2006; **28**:121–132.
11 Kobayashi N, Yoshida K, Nakano S, Ohno T, Honda T, Tsubokou Y, *et al.* Cardioprotective mechanisms of eplerenone on cardiac performance and remodeling in failing rat hearts. *Hypertension* 2006; **47**:671–679.
12 Kobayashi N, Hara K, Tojo A, Onozato ML, Honda T, Yoshida K, *et al.* Eplerenone shows renoprotective effect by reducing LOX-1-mediated adhesion molecule, PKCepsilon-MAPK-p90RSK, and Rho-kinase pathway. *Hypertension* 2005; **45**:538–544.
13 Nagase M, Shibata S, Yoshida S, Nagase T, Gotoda T, Fujita T. Podocyte injury underlies the glomerulopathy of Dahl salt-hypertensive rats and is reversed by aldosterone blocker. *Hypertension* 2006; **47**:1084–1093.
14 Nagata K, Obata K, Xu J, Ichihara S, Noda A, Kimata H, *et al.* Mineralocorticoid receptor antagonism attenuates cardiac hypertrophy and failure in low-aldosterone hypertensive rats. *Hypertension* 2006; **47**:656–664.
15 Ohtani T, Ohta M, Yamamoto K, Mano T, Sakata Y, Nishio M, *et al.* Elevated cardiac tissue level of aldosterone and mineralocorticoid receptor in diastolic heart failure: beneficial effects of mineralocorticoid receptor blocker. *Am J Physiol Regul Integr Comp Physiol* 2007; **292**:R946–R954.
16 Onozato ML, Tojo A, Kobayashi N, Goto A, Matsuoka H, Fujita T. Dual blockade of aldosterone and angiotensin II additively suppresses TGF-beta and NADPH oxidase in the hypertensive kidney. *Nephrol Dial Transplant* 2007; **22**:1314–1322.
17 Takeda Y, Zhu A, Yoneda T, Usukura M, Takata H, Yamagishi M. Effects of aldosterone and angiotensin II receptor blockade on cardiac angiotensinogen and angiotensin-converting enzyme 2 expression in Dahl salt-sensitive hypertensive rats. *Am J Hypertens* 2007; **20**:1119–1124.
18 Aoi W, Niisato N, Miyazaki H, Marunaka Y. Flavonoid-induced reduction of ENaC expression in the kidney of Dahl salt-sensitive hypertensive rat. *Biochem Biophys Res Commun* 2004; **315**:892–896.
19 Aoi W, Niisato N, Sawabe Y, Miyazaki H, Tokuda S, Nishio K, *et al.* Abnormal expression of ENaC and SGK1 mRNA induced by dietary sodium in Dahl salt-sensitively hypertensive rats. *Cell Biol Int* 2007; **31**:1288–1291.
20 Aoi W, Niisato N, Sawabe Y, Miyazaki H, Marunaka Y. Aldosterone-induced abnormal regulation of ENaC and SGK1 in Dahl salt-sensitive rat. *Biochem Biophys Res Commun* 2006; **341**:376–381.
21 Teiwes J, Toto RD. Epithelial sodium channel inhibition in cardiovascular disease. A potential role for amiloride. *Am J Hypertens* 2007; **20**:109–117.
22 Cragoe EJ Jr, Woltersdorf OW Jr, Bicking JB, Kwong SF, Jones JH. Pyrazine diuretics. II. N-amidino-3-amino-5-substituted 6-halopyrazinecarboxamides. *J Med Chem* 1967; **10**:66–75.
23 Kleyman TR, Cragoe EJ Jr. Amiloride and its analogs as tools in the study of ion transport. *J Membr Biol* 1988; **105**:1–21.
24 Kleyman TR, Cragoe EJ Jr. The mechanism of action of amiloride. *Semin Nephrol* 1988; **8**:242–248.
25 Nagase M, Kaname S, Nagase T, Wang G, Ando K, Sawamura T, *et al.* Expression of LOX-1, an oxidized low-density lipoprotein receptor, in experimental hypertensive glomerulosclerosis. *J Am Soc Nephrol* 2000; **11**:1826–1836.
26 Grunder S, Zagato L, Yagil C, Yagil Y, Sassard J, Rossier BC. Polymorphisms in the carboxy-terminus of the epithelial sodium channel in rat models for hypertension. *J Hypertens* 1997; **15**:173–179.
27 Huang H, Pravenec M, Wang JM, Kren V, St LE, Szpirer C, *et al.* Mapping and sequence analysis of the gene encoding the beta subunit of the epithelial sodium channel in experimental models of hypertension. *J Hypertens* 1995; **13**:1247–1251.

28 Shehata MF, Leenen FH, Tesson F. Sequence analysis of coding and 3′ and 5′ flanking regions of the epithelial sodium channel alpha, beta, and gamma genes in Dahl S versus R rats. *BMC Genet* 2007; **8**:35.

29 Yasuhara A, Wada J, Malakauskas SM, Zhang Y, Eguchi J, Nakatsuka A, *et al.* Collectrin is involved in the development of salt-sensitive hypertension by facilitating the membrane trafficking of apical membrane proteins via interaction with soluble N-ethylmaleiamide-sensitive factor attachment protein receptor complex. *Circulation* 2008; **118**:2146–2155.

30 Hughey RP, Bruns JB, Kinlough CL, Harkleroad KL, Tong Q, Carattino MD, *et al.* Epithelial sodium channels are activated by furin-dependent proteolysis. *J Biol Chem* 2004; **279**:18111–18114.

31 Carattino MD, Passero CJ, Steren CA, Maarouf AB, Pilewski JM, Myerburg MM, *et al.* Defining an inhibitory domain in the alpha-subunit of the epithelial sodium channel. *Am J Physiol Renal Physiol* 2008; **294**:F47–F52.

32 Bruns JB, Carattino MD, Sheng S, Maarouf AB, Weisz OA, Pilewski JM, *et al.* Epithelial Na+ channels are fully activated by furin- and prostasin-dependent release of an inhibitory peptide from the gamma-subunit. *J Biol Chem* 2007; **282**:6153–6160.

33 Passero CJ, Mueller GM, Rondon-Berrios H, Tofovic SP, Hughey RP, Kleyman TR. Plasmin activates epithelial Na+ channels by cleaving the gamma subunit. *J Biol Chem* 2008; **283**:36586–36591.

34 Carattino MD, Hughey RP, Kleyman TR. Proteolytic processing of the epithelial sodium channel gamma subunit has a dominant role in channel activation. *J Biol Chem* 2008; **283**:25290–25295.

35 Mok SC, Chao J, Skates S, Wong K, Yiu GK, Muto MG, *et al.* Prostasin, a potential serum marker for ovarian cancer: identification through microarray technology. *J Natl Cancer Inst* 2001; **93**:1458–1464.

36 Svenningsen P, Bistrup C, Friis UG, Bertog M, Haerteis S, Krueger B, *et al.* Plasmin in nephrotic urine activates the epithelial sodium channel. *J Am Soc Nephrol* 2009; **20**:299–310.

37 Maekawa A, Kakizoe Y, Miyoshi T, Wakida N, Ko T, Shiraishi N, *et al.* Camostat mesilate inhibits prostasin activity and reduces blood pressure and renal injury in salt-sensitive hypertension. *J Hypertens* 2009; **27**:181–189.

38 Oda M, Ino Y, Nakamura K, Kuramoto S, Shimamura K, Iwaki M, *et al.* Pharmacological studies on 6-amidino-2-naphthyl[4-(4,5-dihydro-1H-imidazol-2-yl)amino] benzoate dimethane sulfonate (FUT-187). I: Inhibitory activities on various kinds of enzymes in vitro and anticomplement activity in vivo. *Jpn J Pharmacol* 1990; **52**:23–34.

39 Coote K, therton-Watson H, Sugar R, Young A, kenzie-Beevor A, Gosling M, *et al.* Camostat attenuates airway ENaC function in vivo through the inhibition of a Channel Activating Protease. *J Pharmacol Exp Ther* 2009.

40 Sepehrdad R, Chander PN, Oruene A, Rosenfeld L, Levine S, Stier CT Jr. Amiloride reduces stroke and renalinjury in stroke-prone hypertensive rats. *Am J Hypertens* 2003; **16**:312–318.

41 Mirkovic S, Seymour AM, Fenning A, Strachan A, Margolin SB, Taylor SM, *et al.* Attenuation of cardiac fibrosis by pirfenidone and amiloride in DOCA-salt hypertensive rats. *Br J Pharmacol* 2002; **135**:961–968.

42 Campbell SE, Janicki JS, Matsubara BB, Weber KT. Myocardial fibrosis in the rat with mineralocorticoid excess. Prevention of scarring by amiloride. *Am J Hypertens* 1993; **6 (6 Pt 1)**:487–495.

43 O'Connor PM, Lu L, Schreck C, Cowley AW Jr. Enhanced amiloride-sensitive superoxide production in renal medullary thick ascending limb of Dahl salt-sensitive rats. *Am J Physiol Renal Physiol* 2008; **295**:F726–F733.

44 Hong NJ, Garvin JL. Flow increases superoxide production by NADPH oxidase via activation of Na-K-2Cl cotransport and mechanical stress in thick ascending limbs. *Am J Physiol Renal Physiol* 2007; **292**:F993–F998.

Camostat mesilate inhibits prostasin activity and reduces blood pressure and renal injury in salt-sensitive hypertension

Ai Maekawa*, Yutaka Kakizoe*, Taku Miyoshi, Naoki Wakida, Takehiro Ko, Naoki Shiraishi, Masataka Adachi, Kimio Tomita and Kenichiro Kitamura

Prostasin, a glycosylphosphatidylinositol-anchored serine protease, regulates epithelial sodium channel (ENaC) activity. Sodium reabsorption through ENaC in distal nephron segments is a rate-limiting step in transepithelial sodium transport. Recently, proteolytic cleavage of ENaC subunits by prostasin has been shown to activate ENaC. Therefore, we hypothesized that serine protease inhibitors could inhibit ENaC activity in the kidney, leading to a decrease in blood pressure. We investigated the effects of camostat mesilate, a synthetic serine protease inhibitor, and FOY-251, an active metabolite of camostat mesilate, on sodium transport in the mouse cortical collecting duct cell line (M-1 cells) and on blood pressure in Dahl salt-sensitive rats. Treatment with camostat mesilate or FOY-251 decreased equivalent current (I_{eq}) in M-1 cells in a dose-dependent manner and inhibited the protease activity of prostasin *in vitro*. Silencing of the prostasin gene also reduced equivalent current in M-1 cells. The expression level of prostasin protein was not changed by application of camostat mesilate or FOY-251 to M-1 cells. Oral administration of camostat mesilate to Dahl salt-sensitive rats fed a high-salt diet resulted in a significant decrease in blood pressure with elevation of the urinary Na/K ratio, decrease in serum creatinine, reduction in urinary protein excretion, and improvement of renal injury markers such as collagen 1, collagen 3, transforming growth factor-β1, and nephrin. These findings suggest that camostat mesilate can decrease ENaC activity in M-1 cells probably through the inhibition of prostasin activity, and that camostat mesilate can have beneficial effects on both hypertension and kidney injury in Dahl salt-sensitive rats. Camostat mesilate might represent a new class of antihypertensive drugs with renoprotective effects in patients with salt-sensitive hypertension. *J Hypertens* 27:181–189 © 2009 Wolters Kluwer Health | Lippincott Williams & Wilkins.

Journal of Hypertension 2009, 27:181–189

Keywords: epithelial sodium channel, prostasin, renal injury, salt-sensitive hypertension, serine protease inhibitor

Abbreviations: CM, camostat mesilate; DS, Dahl salt-sensitive; ENaC, epithelial sodium channel; EVOM, ohm/volt meter; FOY-251, 4-(4-guanidinobenzoloxy) phenylacetate methanesulfonate; GPI, glycosylphosphatidylinositol; HS, high salt; I_{eq}, equivalent current; NM, nafamostat mesilate; PAC, plasma aldosterone concentration; pfu, plaque-forming units; PRA, plasma renin activity; QAR-MCA, N-t-Boc-Gln-Ala-Arg-7-amido-4-methyl coumarin; R_{te}, transepithelial resistance; SBP, systolic blood pressure; STI, soybean trypsin inhibitor; TCA, trichloroacetic acid; V_{te}, transepithelial voltage

Department of Nephrology, Kumamoto University Graduate School of Medical Sciences, Kumamoto, Japan

Correspondence to Kenichiro Kitamura, MD, PhD, Associate Professor, Department of Nephrology, Kumamoto University Graduate School of Medical Sciences, 1-1-1 Honjo, Kumamoto 860-8556, Japan
Tel: +81 96 373 5164; fax: +81 96 366 8458; e-mail: ken@gpo.kumamoto-u.ac.jp

*These authors contributed equally to this work.

Received 21 March 2008 **Revised** 23 August 2008
Accepted 25 August 2008

Introduction

Proteases are involved in numerous essential biological processes including blood clotting, controlled cell death, and tissue differentiation. Prostasin is a glycosylphosphatidylinositol (GPI)-anchored and/or secreted serine protease purified from human seminal fluid [1], expressed in kidney, prostate, liver, lung, pancreas, colon, and present in urine [2]. Our and other laboratories have demonstrated that prostasin increases epithelial sodium channel (ENaC) activity when the two are coexpressed in *Xenopus* oocytes [3,4]. Sodium reabsorption through ENaC in the distal nephron segment is the first and rate-limiting step in transepithelial sodium transport [5]. This step therefore plays an important role in the regulation of sodium balance, extracellular fluid volume, and blood pressure (BP) by the kidney. The fact that gain-of-function mutations of ENaC are found in Liddle's syndrome strongly supports the contribution of ENaC in the pathogenesis of salt-sensitive hypertension [6]. ENaC is composed of three homologous subunits, α, β, and γ [7]. Several lines of evidence strongly suggest that prostasin plays a pivotal role in the activation of ENaC [3,8,9]. Hughey *et al.* [10] demonstrated that the proteolytic processing of ENaC α and γ subunits was required for channel maturation. Bruns *et al.* [11] showed that dual cleavage of the γ subunit by prostasin and furin releases a 43-amino acid peptide that is a potent inhibitor of ENaC, leading to an increase in the open probability of the channel. These findings strongly indicate a primary role for the proteolytic activity of prostasin in the activation of ENaC and consequently in the regulation of sodium handling, fluid volume, and BP by the kidney.

Several investigators showed that a selective serine protease inhibitor, aprotinin, which is a potent inhibitor of prostasin, reduced the ENaC activity in heterologous expression systems [3,4]. Previously, we found that nafamostat mesilate, a synthetic serine protease inhibitor,

0263-6352 © 2009 Wolters Kluwer Health | Lippincott Williams & Wilkins DOI:10.1097/HJH.0b013e328317a762

reduced renal sodium reabsorption in rats [12]. The Dahl salt-sensitive rat is a well known model of salt-sensitive hypertension. Rapid progression of hypertension, severe proteinuria, and renal failure are found in high salt fed Dahl salt-sensitive rats, whose renal histopathological manifestations include glomerulosclerosis and renal arterial injury [13]. Several mechanisms of salt-sensitive hypertension in Dahl salt-sensitive rats have been postulated, and most of them are related to sodium metabolism [14,15]. Moreover, Aoi *et al.* [16] reported paradoxical elevation of αENaC mRNA expression in the kidneys of Dahl salt-sensitive rats despite suppressed plasma aldosterone concentration (PAC) by the high-salt diet. A number of researchers showed beneficial effects of antihypertensive drugs such as renin–angiotensin system inhibitors on hypertension or renal injury in Dahl salt-sensitive rats fed with high-salt diets [17,18]. However, the effect of systemic administration of ENaC inhibitors or serine protease inhibitors on hypertension has not been reported in Dahl salt-sensitive rats.

Therefore, we hypothesized that serine protease inhibitors can reduce BP through the inhibition of prostasin and ENaC activity in the kidney and investigated the effect of camostat mesilate, an orally active synthetic serine protease inhibitor, on prostasin activity, the amiloride-sensitive sodium current in cultured renal epithelial cells, and BP in salt-sensitive hypertension in Dahl rats. When camostat mesilate is given orally to humans, it is absorbed by the gastrointestinal tract as camostat mesilate or its active metabolite, 4-(4-guanidinobenzoloxy) phenylacetate methanesulfonate (FOY-251). Because the inhibitory effect of FOY-251 is very similar to that of camostat mesilate, we also determined the effect of FOY-251 on prostasin activity and the amiloride-sensitive sodium current in cultured renal epithelial cells.

Methods

Cell culture

Mouse cortical collecting duct cells (M-1 cells) were the kind gift of Dr L. Lee Hamm (Tulane University). Cells were cultured in plastic dishes and were maintained as described previously [19,20]. Experiments were performed when cells were confluent, and both serum and other ingredients were removed 24 h before experiments. All studies described in this paper were performed on cells between the 5th and 20th passages.

Electrophysiological measurements

For electrophysiological measurements, cells were seeded onto semi-permeable polycarbonate membranes (12 mm in diameter) (Transwell; Corning, Lowell, Massachusetts, USA). Transepithelial voltage (V_{te}) and resistance (R_{te}) were measured with an ohm/volt meter (EVOM; World Precision Instruments Inc, Sarasota, Florida, USA) as described previously [20]. The equivalent current (I_{eq}) was calculated as the ratio of V_{te} to R_{te} and was normalized by dividing I_{eq} by the surface area (113 mm^2) of active membrane.

Purification of recombinant human prostasin

A cDNA for recombinant human prostasin was created by inserting an enterokinase cleavage site, Asp–Asp–Asp–Asp–Lys, between the light chain and heavy chain and by replacing the C-terminal membrane anchoring domain with a 6 × His tag, so that the recombinant protein could be secreted as a pro-protein and could be activated by exogenous enterokinase treatment. The cDNA was subcloned into a transfer vector, pM00001 (Katakura Industries, Saitama, Japan). Linearized hybrid baculovirus DNA 'Bac-Duo' (Katakura Industries) was cotransfected with recombinant plasmid into a *Spodoptera frugiperda* cell line, SF21AE. Three days after transfection, the culture supernatants containing recombinant human prostasin virus were harvested and subjected to the standard plaque purification methods. Silkworm larvae at the early stage of the fifth instar were infected with 9×10^4 plaque-forming units (pfu) of recombinant virus. On the fifth day after infection, hemolymph-containing recombinant human prostasin was harvested by cutting off several abdominal legs from each larva. The hemolymph was collected in 0.1 mol/l phosphate buffer, pH 6.8, supplemented with 0.1% N-phenylthiourea. Recombinant human prostasin was purified using a Ni-sepharose column (HisTrap HP; GE Healthcare Bio-Sciences, Piscataway, New Jersey, USA) and ion exchange column (Resourse Q; GE Healthcare Bio-Sciences) with AKTA prime (GE Healthcare Bio-Sciences). Purified recombinant prostasin was incubated with enterokinase (EK Max; Invitrogen, Carlsbad, California, USA) for 16 h at 37°C to generate an enzymatically active recombinant human prostasin by cleaving the enterokinase cleavage site between the light and heavy chains. Sixteen hours after incubation, enterokinase was removed from the reaction mixture by using an enterokinase removal kit (Sigma, St Louis, Missouri, USA). Activation of prostasin was assessed using an enzymatic assay as described below.

Purification of recombinant human prostasin

Activated recombinant human prostasin was a synthetic substrate, N-t-Boc-Gln-Ala-Arg-7-amido-4-methyl coumarin (QAR-MCA), and was purchased from Peptide Institute (Osaka, Japan), and camostat mesilate was a gift of Ono Pharmaceutical Co., Ltd. (Osaka, Japan). One microliter of camostat mesilate ($0–10^{-4}$ mol/l) was preincubated with 15 μl of prostasin (1 μmol/l) for 30 min at room temperature. The reaction mixture was then added to 80 μl of 50 mmol/l Tris-HCl (pH 7.6) containing the QAR-MCA substrate (final concentration: 1 mmol/l in 96-well microtiter plates (Costar 3903; Costar, Cambridge, Massachusetts, USA). The velocity of substrate hydrolysis was measured by using a fluorescent microplate reader (Ultra Evolution; Tecan, Zurich, Switzerland) at excitation 360 nm and emission 465 nm. The residual activity of

prostasin (velocity of inhibited enzyme reaction/velocity of uninhibited enzyme reaction) was plotted vs. camostat mesilate concentration.

RNA isolation, reverse transcription, and real-time PCR analysis

Total RNA was extracted from M-1 cells using the RNeasy Mini Kit (Qiagen, Hilden, Germany). Five micrograms of total RNA was reverse transcribed to cDNA with oligo (dT) and random primers using QuantiTect Reverse Transcription Kit (Invitrogen). TaqMan probes for mouse prostasin, rat collagen type I, rat collagen type III, rat transforming growth factor-β1 (TGF-β1), rat nephrin and glyceraldehyde 3-phosphate dehydrogenase (GAPDH) were purchased from Applied Biosystems (Foster City, California, USA). Real-time PCR was performed with an ABI PRISM 7900 Sequence Detector System (Applied Biosystems). Statistical analysis of results was performed with the Δcycle threshold value (cycle threshold$_{\text{gene of interest}}$ − cycle threshold $_{\text{GAPDH}}$). Relative gene expression was obtained using the ΔΔcycle threshold method (cycle threshold$_{\text{sample}}$ − cycle threshold$_{\text{calibrator}}$).

Protein preparation and immunoblotting

Twenty-four hours after incubation under experimental conditions, culture medium was collected and centrifuged at 1200*g* to pellet cell debris. Total protein in the culture media was precipitated using TCA (final concentration, 15%). Samples were centrifuged at 12 000*g*, and the pellets were washed three times with ice-cold 80% acetone. The precipitated proteins were dried and solubilized at 100°C for 5 min in 1 × TCA buffer (200 mmol/l unbuffered Tris, 1% SDS, 10% glycerol, and 1% β-mercaptoethanol). For preparation of the membrane fraction of M-1 cells, confluent M-1 cells were washed twice with phosphate-buffered saline, scraped into lysis buffer (25 mmol/l Tris-HCl, pH 7.5, 0.61 μmol/l aprotinin, 8.4 μmol/l leupeptin, 1 mmol/l phenylmethylsulfonylfluoride, and 5.8 μmol/l pepstatin A), and lysed in a glass Dounce homogenizer. The homogenate was centrifuged at 800*g* to remove nuclei, and the supernatant was centrifuged at 12 000*g* to separate the membrane and cytosolic fractions. The membrane fraction was then dissolved in radioimmuno precipitation assay buffer (50 mmol/l Tris-HCl, pH 7.5, 150 mmol/l NaCl, 0.1% SDS, 0.5% deoxycholate, 1% (v/v) Triton-X 100, 2 mmol/l EDTA, 0.61 μmol/l aprotinin, 8.4 μmol/l leupeptin, 1 mmol/l phenylmethylsulfonylfluoride, and 5.8 μmol/l pepstatin A). All procedures were performed at 4°C. Samples were electroporated on 12% SDS–polyacrylamide gels and transferred onto nitrocellulose filters. After blocking with 50 g/l nonfat dry milk, blots were probed with a monoclonal antibody against prostasin (BD Biosciences Pharmingen, San Diego, California, USA) in Can Get signal solution I (TOYOBO, Osaka, Japan) for 16 h, followed by a secondary antibody (goat antimouse immunoglobulin G conjugated with horseradish peroxidase) in Can Get Signal solution II (TOYOBO) for 1 h at room temperature. Bands were visualized using chemiluminescence substrate (ECL; Amersham Pharmacia Biotech, Buckinghamshire, UK) before exposure to X-ray film. The band densities were quantitated by densitometry (Densitograph 4.0; ATTO, Tokyo, Japan).

Application of prostasin small interfering RNA

M-1 cells were transfected with prostasin small interfering RNA (siRNA) (Silencer Predesigned siRNA, siRNA ID # 175650, Ambion Inc., Austin, Texas, USA) or control siRNA (Silencer Negative Control siRNA, siRNA ID # 4635, Ambion Inc.) by using Lipofectamine 2000 (Invitrogen) according to the manufacture's instructions. Twenty-four hours after transfection, cells were deprived of serum for 48 h, and I_{eq} was measured as described above.

Animals

All the animal procedures were in accordance with the guidelines for care and use of laboratory animals approved by Kumamoto University. Four-week-old Dahl salt-sensitive rats ($n = 16$) were purchased from Kyudo Co., Ltd. (Tosu, Japan). Rats were divided into two groups; one group ($n = 8$) was fed with a high-salt diet (8% NaCl) (high-salt rats) and the other group ($n = 8$) was fed with high-salt diet containing 0.1% camostat mesilate (camostat mesilate rats) for 3 weeks. Systolic blood pressure (SBP) was measured every week under awake conditions by the tail–cuff method (MK-2000; Muromachi Kikai Co., Ltd., Osaka, Japan). Twenty-four-hour urine samples were collected in metabolic cages every week, and urine volume, electrolytes, creatinine, and total protein were measured. After 3 weeks, rats were decapitated and blood samples were collected. The hearts and kidneys were weighed, and whole kidneys were removed and immediately homogenized with T-PER solution (Pierce Biotechnology, Rockford, Illinois, USA). Electrolytes, creatinine, plasma renin activity (PRA), and PAC were measured commercially (SRL, Tokyo, Japan). Urinary concentrations of camostat mesilate and FOY-251 were determined by high-performance liquid chromatography.

Statistical analysis

Statistical significance was evaluated using the two-tailed, paired Student's *t*-test for comparisons between two means or analysis of variance followed by the Newman–Keuls method for more than two means. A P value of less than 0.05 was regarded as statistically significant. Results are reported as mean ± SD.

Results

Effect of camostat mesilate and FOY-251 on equivalent current in M-1 cells

M-1 cells were plated onto permeable supports. Three to four days after seeding, M-1 cells developed R_{te} ranging up to more than 200 Ω. Cells were then deprived of serum

Fig. 1

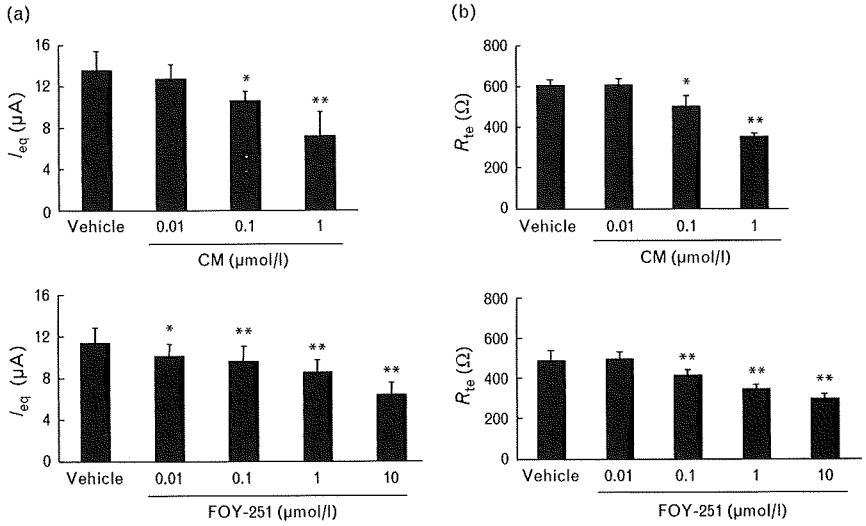

Effects of camostat mesilate and FOY-251 on equivalent current and resistance in M-1 cells. M-1 cells were cultured on semi-permeable membrane, serum deprived for 24 h, and treated with 0.01–1 μmol/l camostat mesilate or 0.01–10 μmol/l FOY-251 from the apical side. After 24-h incubation, transepithelial voltage (V_{te}) and resistance (R_{te}) (b) were measured with a volt–ohm meter. I_{eq} (a) was determined as the ratio of V_{te} to R_{te} and was normalized by dividing I_{eq} by the surface area (1.13 mm^2) of active membrane. Data are expressed as mean ± SD ($n = 6$). CM, camostat mesilate; I_{eq}, equivalent current; R_{te}, resistance. *$P < 0.05$ vs. vehicle; **$P < 0.001$ vs. vehicle.

for 24 h. Amiloride-sensitive I_{eq} was measured 24 h after the addition of vehicle, camostat mesilate or FOY-251 to the luminal side of the cell monolayers. As shown in Fig. 1a, treatment with camostat mesilate significantly decreased I_{eq} in M-1 cells in a dose-dependent manner over a range of 0–1 μmol/l. Similarly, treatment with FOY-251 also represented a dose-dependent inhibition of I_{eq} in M-1 cells. Intriguingly, we also found a dose-dependent decrease in R_{te} by camostat mesilate and FOY-251 in M-1 cells (Fig. 1b).

Inhibition of proteolytic activity of prostasin by camostat mesilate and FOY-251

Because prostasin is a primary regulator of ENaC, we hypothesized that camostat mesilate or FOY-251 or both reduced sodium transport by inhibiting prostasin activity and tested the effect of camostat mesilate and FOY-251 on the proteolytic activity of prostasin *in vitro*. As shown in Fig. 2, both camostat mesilate and FOY-251 inhibited the proteolytic activity of prostasin. Inhibitory rates of camostat mesilate on prostasin activity were 7.6 ± 0.2, 42.0 ± 0.3, and 85.3 ± 0.7% with concentrations of 0.1, 1, and 10 μmol/l, respectively. FOY-251 also inhibited prostasin activity by 3.2 ± 0.5, 6.1 ± 3.2, 34.4 ± 1.0, and 81.3 ± 0.6% with concentrations of 0.1, 1, 10, and 100 μmol/l, respectively. The effect of camostat mesilate and FOY-251 on prostasin activity displayed a clear dose dependency. The rates of reduction in I_{eq} by camostat mesilate and FOY-251 were comparable to that of prostasin activity, indicating that camostat mesilate and FOY-251 inhibited ENaC activity through the suppression of proteolytic activity of prostasin in M-1 cells.

Effect of prostasin gene silencing on equivalent current in M-1 cells

M-1 cells were transfected with prostasin siRNA or negative control siRNA. As shown in Fig. 3a, prostasin siRNA reduced the expression of prostasin at the protein level (39 ± 5%). To determine the contribution of prostasin to transepithelial sodium transport in M-1 cells, electrophysiological measurements were performed using EVOM. Gene silencing of prostasin suppressed I_{eq} by 69 ± 6% in M-1 cells (Fig. 3b). As was the case with camostat mesilate treatment, silencing of the prostasin gene also reduced R_{te} in M-1 cells by 41 ± 3% (Fig. 3c). These data suggest a substantial contribution of prostasin to the regulation of sodium transport in M-1 cells and indicate that the amount of prostasin as well as the activity of prostasin has a significant influence on ENaC activity.

Effect of camostat mesilate and FOY-251 on prostasin expression in M-1 cells

To determine the effect of camostat mesilate on the expression of prostasin at the protein level, M-1 cells were treated with 1 μmol/l camostat mesilate or 10 μmol/l FOY-251 for 24 h, and both GPI-anchored and secreted forms of prostasin were evaluated by immunoblotting using a specific monoclonal antibody against prostasin. As shown in Fig. 4a–d, the expression of both forms of prostasin was not significantly affected by camostat mesilate and FOY-251 treatment. These findings indicate that the decrease in I_{eq} caused by camostat mesilate and FOY-251 is not mediated by the suppression of prostasin expression in M-1 cells.

Fig. 2

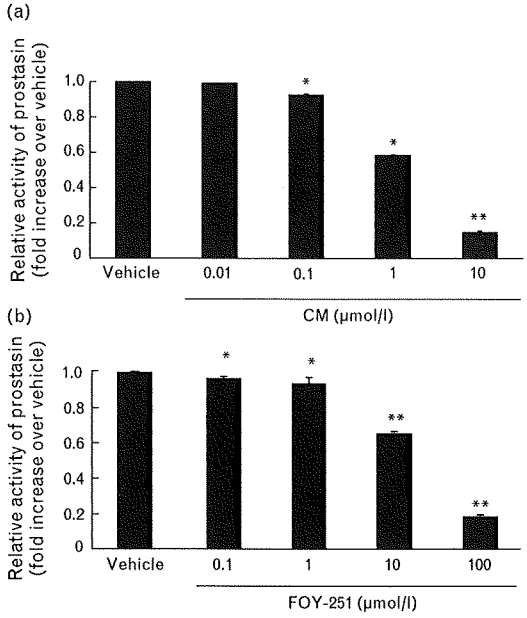

Effect of camostat mesilate and FOY-251 on the enzymatic activity of prostasin. Recombinant human prostasin was treated with camostat mesilate (0.01–10 μmol/l) (a) or FOY-251 (0.1–100 μmol/l) (b) for 30 min at room temperature. Then, QAR-MCA (1 mmol/l), a synthetic substrate for prostasin, was added. Proteolytic activity was measured by using a fluorescent microplate reader. Values are expressed as fold increase over vehicle. Data are expressed as mean ± SD ($n = 3$). CM, camostat mesilate. $^{*}P < 0.05$ vs. vehicle; $^{**}P < 0.001$ vs. vehicle.

Effect of camostat mesilate on hypertension and renal injury in Dahl salt-sensitive rats

Because we found that camostat mesilate markedly suppressed ENaC activity in M-1 cells, we next investigated whether camostat mesilate could reduce BP in Dahl salt-sensitive rats in which ENaC is demonstrated to be highly active. SBP in high-salt rats began to increase at day 7 and reached over 200 mmHg at day 21. SBP in camostat mesilate rats also tended to increase; however, camostat mesilate significantly reduced SBP at days 14 and 21 (high salt vs. camostat mesilate; 180 ± 13 vs. 154 ± 10 mmHg at day 14, $P < 0.001$, and 207 ± 12 vs. 157 ± 12 mmHg at day 21, $P < 0.001$) (Fig. 5a). In addition, urinary protein was strikingly reduced by camostat mesilate treatment (Fig. 5b), resulting in an increase in serum albumin levels in camostat mesilate rats. Camostat mesilate also improved serum creatinine levels and creatinine clearance, suggesting a renoprotective effect probably due to the reduction in both BP and proteinuria. Body weight and food intake were almost identical in each group during the experimental period. Kidney weights were significantly reduced in camostat mesilate rats compared with those in high-salt rats. Serum Na and K levels, PRA, and PAC were not significantly different between the two groups. Urine volume and urinary sodium excretion were not different between them. Interestingly, the urinary Na/K ratio was significantly increased in camostat mesilate rats (high salt vs. camostat mesilate; 6.4 ± 0.6 vs. 7.0 ± 0.3, $P < 0.05$), suggesting that camostat mesilate indeed inhibited ENaC activity *in vivo*. We also determined the urinary concentration of camostat mesilate and FOY-251 after 3 weeks of administration. Camostat mesilate was not detectable in urine, but a sufficient amount of FOY-251 was detected (FOY-251, 10.51 ± 2.33 μmol/l). Characteristics of each experimental group including blood and urine parameters at day 21 are summarized in Table 1. Real-time PCR analysis revealed that the expression of mRNA coding for renal injury markers such as collagen type I, collagen type III, and TGF-β1 were all significantly decreased, and the expression of nephrin, a reciprocal marker of

Fig. 3

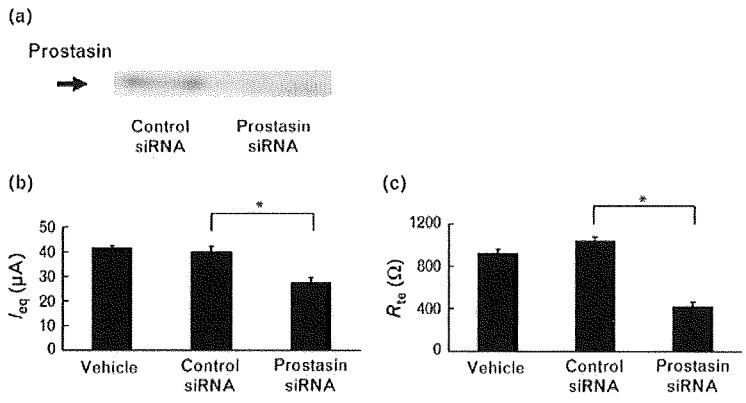

Effect of gene silencing of prostasin on equivalent current and resistance in M-1 cells. M-1 cells were transfected with negative control siRNA or prostasin siRNA. Twenty-four hours after transfection, cells were deprived of serum for 48 h. (a) Seventy-two hours after incubation with siRNA, M-1 cells were harvested, and expression of prostasin protein was determined by immunoblotting. The blots shown are representative of four separate experiments. (b and c) I_{eq} and R_{te} in M-1 cells were measured using an ohm/volt meter 72 h after incubation with siRNA. Data are expressed as mean ± SD ($n = 12$). I_{eq}, equivalent current; R_{te}, resistance; siRNA, small interfering RNA. $^{*}P < 0.001$ vs. control siRNA.

Fig. 4

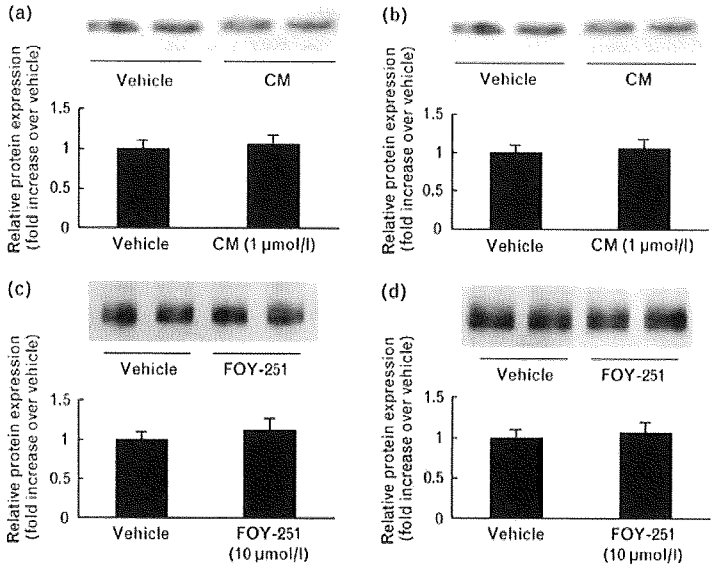

Effect of camostat mesilate and FOY-251 on prostasin protein expression in M-1 cells. M-1 cells were deprived of serum for 24 h and treated with camostat mesilate or FOY-251 for 24 h. Four milliliters of culture medium were TCA precipitated, and membrane fraction proteins were harvested. Both TCA-precipitated medium (a, c) and 10 μg of membrane fraction (b, d) were subjected to SDS-polyacrylamide gel electrophoresis. The expression of prostasin protein was evaluated by immunoblotting using an anti-prostasin monoclonal antibody (upper panel). The blots shown are representative of five separate experiments. The graph shows the quantification of the band intensity for prostasin protein (lower panel). Results are expressed as mean ± SD ($n = 5$). CM, camostat mesilate.

podocyte injury, was markedly increased in camostat mesilate rats (Fig. 5c).

Discussion

In the current studies, we describe the following findings: camostat mesilate and FOY-251 directly inhibited prostasin activity *in vitro* and decreased the sodium current in M-1 cells; knockdown of prostasin gene expression significantly diminished I_{eq} in M-1 cells to a similar extent as camostat mesilate; and oral administration of camostat mesilate substantially improved hypertension and renal injury in Dahl salt-sensitive rats fed a high-salt diet. These results suggest that camostat mesilate reduces ENaC activity probably through the inhibition of prostasin in M-1 cells and displays antihypertensive and renoprotective effects on salt-sensitive hypertension in Dahl salt-sensitive rats.

Previous reports showed that aprotinin, a serine protease inhibitor, decreased I_{eq} in A6 cells, JME/CF15 nasal epithelial cells, and M-1 cells where prostasin is distinctly expressed [4,8], suggesting that inhibition of endogenous serine protease(s), including prostasin, in these epithelial cells leads to a decrease in I_{eq}. In the present study, we demonstrated that camostat mesilate and FOY-251 also significantly reduced I_{eq} in M-1 cells. Because prostasin activity is inhibited by serine protease inhibitors such as aprotinin, benzamidine, antipain, and leupeptin [1], it is reasonable to speculate that camostat mesilate and FOY-251 inhibit prostasin activity and, subsequently, ENaC activity. Indeed, enzyme activity assays of prostasin using a synthetic substrate (QAR-MCA) revealed a significant inhibitory effect of camostat mesilate and FOY-251 on prostasin activity *in vitro*, indicating that they are potent inhibitors of prostasin. siRNA-mediated gene silencing of prostasin in M-1 cells also resulted in a significant decrease in I_{eq}, and the rate of reduction in I_{eq} by siRNA was comparable to that by camostat mesilate and FOY-251. Because camostat mesilate and FOY-251 had no effect on the protein abundance of prostasin (Fig. 4a–d), the inhibition of proteolytic activity of prostasin is presumably responsible for the reduction in I_{eq} in M-1 cells. Another possible mechanism by which camostat mesilate and FOY-251 could reduce sodium transport in M-1 cells is through the inhibition of prostasin zymogen activation. Serine proteases are generally involved in the regulation of zymogen cascades to execute biological activities. In fact, the prostasin proenzyme is activated by cleavage of peptide bonds between light and heavy chains, and the two chains are held together by a disulfide bond [2]. Recently, Netzel-Arnett *et al.* [21] indicated that matriptase, a trypsin-like serine protease expressed in many tissues including the kidney, acts upstream of prostasin in a zymogen activation cascade. Interestingly, camostat mesilate has been shown to markedly repress the proteolytic activity of matriptase [22]. Thus, there is a possibility that camostat mesilate may inhibit prostasin activity through the suppression of prostasin zymogen activation by matriptase, leading to a reduction in sodium transport in M-1 cells.